

AperTO - Archivio Istituzionale Open Access dell'Università di Torino

**Kircherite, a new mineral of the cancrinite-sodalite group with a 36-layer stacking sequence:  
Occurrence and crystal structure.**

**This is the author's manuscript**

*Original Citation:*

*Availability:*

This version is available <http://hdl.handle.net/2318/104603> since

*Published version:*

DOI:10.2138/am.2012.4033

*Terms of use:*

Open Access

Anyone can freely access the full text of works made available as "Open Access". Works made available under a Creative Commons license can be used according to the terms and conditions of said license. Use of all other works requires consent of the right holder (author or publisher) if not exempted from copyright protection by the applicable law.

(Article begins on next page)

This is the author's final version of the contribution published as:

Cámara F; Bellatreccia F; Della Ventura G; Gunter ME; Sebastiani M;  
Cavallo A. Kircherite, a new mineral of the cancrinite-sodalite group with a  
36-layer stacking sequence: Occurrence and crystal structure.. AMERICAN  
MINERALOGIST. 97 pp: 1494-1504.  
DOI: 10.2138/am.2012.4033

The publisher's version is available at:

<http://ammin.geoscienceworld.org/cgi/doi/10.2138/am.2012.4033>

When citing, please refer to the published version.

Link to this full text:

<http://hdl.handle.net/2318/104603>

1 **FIRST REVISION 20/03/2012**

2  
3 **KIRCHERITE, A NEW MINERAL OF THE CANCRINITE - SODALITE GROUP WITH A**  
4 **36-LAYER STACKING SEQUENCE: OCCURRENCE AND CRYSTAL STRUCTURE**

5 **Fernando Cámara<sup>1</sup>**

6 <sup>1</sup> Dipartimento di Scienze della Terra, Università di Torino

7 Via Valperga Caluso 35, 10125 Torino, Italy

8 **Fabio Bellatreccia<sup>2</sup>, Giancarlo Della Ventura<sup>2</sup>**

9 <sup>2</sup> Dipartimento Scienze Geologiche, Università Roma Tre,

10 Largo San Leonardo Murialdo 1, 00146 Rome, Italy

11 **Mickey E. Gunter<sup>3</sup>**

12 <sup>3</sup> Department of Geological Sciences, University of Idaho

13 Moscow Idaho, 83844-3022, USA

14 **Marco Sebastiani<sup>4</sup>**

15 <sup>4</sup> Dipartimento di Ingegneria Meccanica e Industriale, Università Roma Tre

16 Via della Vasca Navale 79, I-00146 Rome, Italy

17 **Andrea Cavallo<sup>5</sup>**

18 <sup>5</sup> Istituto Nazionale di Geofisica e Vulcanologia (I.N.G.V.),

19 Via di Vigna Murata 605, I-00143 Rome, Italy

20 **Corresponding Author:**

21 Fabio Bellatreccia. Dipartimento Scienze Geologiche, Università Roma Tre, Largo San Leonardo Murialdo 1,  
22 I-00146 Roma, Italy

23 e-mail: bellatre@uniroma3.it

24 Tel: +39-06 57 338 068

25 Fax: +39 06 57 338 201

26 Written on IBM compatible computer, MS Word text editor

## ABSTRACT

This paper reports on the occurrence and the crystal structure of kircherite, a new member of the cancrinite-sodalite group of minerals from Valle Biachella, Sacrofano community (Rome, Latium, Italy). The mineral occurs in association with sodalite, biotite, iron oxides, titanite, fluorite and a pyrochlore-group mineral. The groundmass of the ejectum consists essentially of K-feldspar with subordinate plagioclase. Kircherite (3 mm as largest size) is observed within miarolitic cavities of the rock and typically occurs as parallel associations of hexagonal, thin, tabular colorless to light gray transparent crystals; it is non-pleochroic and uniaxial negative, with  $\omega = 1.510(2)$  and  $\varepsilon = 1.502(2)$ .  $D_{\text{calc}}$  is 2.457 g/cm<sup>3</sup>. Kircherite is trigonal with  $a = 12.8770(7)$ ,  $c = 95.244(6)$  Å,  $V = 13677(1)$  Å<sup>3</sup>,  $Z = 1$ . The structure has been refined in the trigonal space group  $R\bar{3}2$ , obtaining a R-value of 8.5% on 8131 reflections with  $I/\sigma I > 2$ . The strongest seven reflections in the X-ray powder pattern are [ $d$  in Å (I %)] ( $hkl$ ): 3.717 (100) (3 0 0), 2.648 (100) (2 1 28; 0 0 36), 3.232 (65) (2 1 19), 3.584 (60) (1 2 14), 3.604 (53) (1 0 25), 3.799 (52) (1 2 11), 3.220 (38) (2 2 0). The single-crystal FTIR spectrum rules out OH groups and shows the presence of H<sub>2</sub>O and CO<sub>2</sub> molecules in the structural cages of the mineral. Chemical analysis gives (in wt%): SiO<sub>2</sub> 32.05, Al<sub>2</sub>O<sub>3</sub> 27.13, FeO 0.07, K<sub>2</sub>O 4.38, CaO 8.75, Na<sub>2</sub>O 13.62, MgO 0.01, MnO 0.02, TiO<sub>2</sub> 0.01, SO<sub>3</sub> 12.87, Cl 0.35, F 0.05. The empirical formula calculated on the basis of  $\Sigma(\text{Si}+\text{Al}) = 216$  apfu is:

$$(\text{Na}_{89.09}\text{Ca}_{31.63}\text{K}_{18.85}\text{Fe}_{0.20}\text{Mn}_{0.06}\text{Mg}_{0.05}\text{Ti}_{0.03})_{\Sigma=139.91}[(\text{Si}_{108.13}\text{Al}_{107.87})_{\Sigma=216.00}\text{O}_{430.00}](\text{SO}_4)_{32.58}\text{Cl}_{2.00}\text{F}_{0.53}\cdot 6.86\text{H}_2\text{O},$$

which corresponds to the ideal formula

$$[\text{Na}_{90}\text{Ca}_{36}\text{K}_{18}]_{\Sigma=144}(\text{Si}_{108}\text{Al}_{108}\text{O}_{432})(\text{SO}_4)_{36}\cdot 6\text{H}_2\text{O}.$$

The structure can be described as a stacking sequence of 36 layers of six-membered rings of tetrahedra along the  $c$  axis. The stacking sequence is ACABCABCABCACBCABCABCABCBCABCABCABCAB..., where A, B and C represent the positions of the rings within the layers. This sequence gives rise to cancrinite, sodalite

and losod cages, alternating along *c*. Sulfate groups occur within the sodalite and losod cages associated by Na, K and Ca. H<sub>2</sub>O groups occur within the cancrinite cages, bonded to Ca and Na cations. Anion groups (SO<sub>4</sub><sup>2-</sup>) in sodalite cages show positional disorder, and so do consequently the extraframework cation sites to them related.

**Keywords:** New minerals, kircherite, ordered interstratified sodalites-cancrinite, crystal structure, IR spectroscopy, mechanical properties.

## INTRODUCTION

The cancrinite group of feldspathoids includes several species structurally characterized by layers of six-membered rings of [SiO<sub>4</sub>] and [AlO<sub>4</sub>] tetrahedra stacked along the crystallographic *c* direction (hereafter 6mR ⊥ [00.1]). The different stacking sequences give rise to different types of structural channels and cages (Bonaccorsi and Merlino 2005). These pores may host several anions and molecular groups, such as H<sub>2</sub>O, Cl, (CO<sub>3</sub>)<sup>2-</sup>, (SO<sub>4</sub>)<sup>2-</sup>, (S<sub>2</sub>)<sup>-</sup>, (S<sub>3</sub>)<sup>-</sup>, (PO<sub>4</sub>)<sup>3-</sup>, (C<sub>2</sub>O<sub>4</sub>)<sup>2-</sup>, CO<sub>2</sub> and extra-framework cations such as Na, K and Ca. The stacking sequence can be simple like ...ABABAB... (where A and B are the positions in successive layers, using the notation of the closest-packed structures) as in cancrinite *sensu stricto*, or can be complex, leading to a variety of species for which sequences of 4, 6, 8, 10, 12, 14, 16, 28, 30, and 33 layers for the *c* translation have been described (for 4 to 16 see Table 2 in Bonaccorsi and Merlino 2005; 28 layers = sacrofanite: Bonaccorsi et al. 2012; 30 layers = biachellaite: Chukanov et al. 2008, Rastsvetaeva and Chukanov 2008; 33 layers = fantappièite: Cámara et al. 2010). Domains with 18 and 24 layer sequences were also observed by transmission electron microscopy (Rinaldi and Wenk 1979). An equal number of layers can also give rise to different sequences, like in marinellite (Bonaccorsi and Orlandi 2003) vs tounkite (Rozenberg et al. 2004), both structures having 12 layers sequences, or to different anion-cation population

of the cages. An example of this latter case is represented by afghanite and alloriite which, although having the same type of framework, differ in having Ca-Cl-Ca-Cl (Ballirano et al. 1997) or Na-H<sub>2</sub>O-Na-H<sub>2</sub>O (Chukanov et al. 2007; Rastsvetaeva et al. 2007) extraframework contents, respectively. Recently, carbobystrite has been described as having the same staking sequence of bystrite (ABAC) but having CO<sub>3</sub> and H<sub>2</sub>O groups instead of S<sup>2-</sup> as in bystrite (Khomyakov et al. 2010).

Kircherite was found -- and donated to us by Mr. L. Mattei (1947 - 2012), a distinguished amateur mineral collector -- within the miarolitic cavities of a holocrystalline volcanic ejectum collected at Valle Biachella, Sacrofano community, in the Sabatini volcanic complex, Latium (Italy). We succeeded to obtain a structural model for this mineral, and a formal proposal was submitted the IMA-NMNC Commission, which approved the species and the name (IMA 2009-086). The name kircherite is for Athanasius Kircher (1602 – 1680), a German Jesuit scholar who published around 40 works, some of which dealt with magnetism, geology, mineralogy and volcanology. Athanasius Kircher was in Rome from 1635 and was the founder of the museum of the *Collegium Romanum* in 1651, hereafter named the *Museum Kircherianum*. It contained collections of Roman, Etruscan, and Egyptian antiquities including mummies and large collections of natural objects such as minerals and precious stones. The refined and analyzed crystal is deposited at the Museum of Mineralogy of the "Sapienza" University of Roma (code number MMUR 33035/1). This paper is dedicated to the memory of Luigi Mattei.

#### **OCCURRENCE, PHYSICAL AND OPTICAL PROPERTIES**

The holocrystalline volcanic ejectum containing kircherite was collected at Valle Biachella, Sacrofano community. Valle Biachella is a small valley on the inner side of the Sacrofano caldera wall, in the eastern sector of the Sabatini volcanic complex which is

located in northern-central Latium about 20 km to the north of Rome. This complex, together with the other Latian volcanic complexes, belongs to the so-called "Roman Ultrapotassic Province." The Sabatini volcanic complex is characterized by an areal, mainly explosive activity, with the emplacement of numerous eruptive centers, which started about 0.6 Ma ago and ended about 0.08 Ma ago. This activity evolved throughout several caldera collapses and the emission of large volumes of pyroclastic products having the alkaline-potassic signature typical of the Roman Ultrapotassic Province. In Valle Biachella outcrops essentially the "Sacrofano upper pyroclastic flow" unit linked to the volcanic activity of the satellite center of Sacrofano (De Rita et al. 1983, 1993 and references therein).

The ejectum, about 15 cm in size, is a granular but compact rock whitish-gray in color. The groundmass consists of interlocking K-feldspar with minor sodalite, plagioclase, brown mica and andraditic garnet. Fluorite, iron oxides, a pyrochlore-group mineral, and a britholite-like phase are the accessory minerals (Fig. 1a and 1b). Kircherite, which occurs within the interstices between the interlocking K-feldspar, occurs as parallel associations of hexagonal thin tabular shaped crystals (Fig. 2a). The morphology of the kircherite crystals results essentially from the combination of the {00.1} pinacoid with the  $\{101; \bar{1}\}$  rhombohedron (Fig. 2b). The maximum size of the crystal groups does not exceed 2 or 3 mm in diameter and up to 1 mm in thickness; the single platelets have a thickness that very rarely exceeds 0.5 mm.

Kircherite appears as transparent to translucent and even opaque in the most altered parts of the material; the luster is greasy to silky and the streak is white. The samples fluoresce light pink under long wave UV and deep red under short wave UV. It is brittle with an uneven fracture and a good cleavage on {00.1}; parting is not observed. The measured density, determined by flotation in a mixture of bromoform-ethanol, is  $D_{\text{meas}} = 2.42 \text{ g/cm}^3$  and the calculated density from the empirical formula is  $D_{\text{calc}} = 2.457 \text{ g/cm}^3$ .

Vickers hardness was measured at the Interdepartmental Laboratory of Electron Microscopy (LIME), Università Roma Tre, by means of a Mitutoyo HM-124 microhardness tester, with an applied load of 10 gf (0.1 N) (duration of force 10 s, other test parameters in accordance with ASTM E384 Standard 2008). The average diagonal of the Vickers indent was measured by a Digital Optical Microscope at a magnification of 1000x. Vickers Hardness Number (VHN) was calculated by the following equation:  $VHN = 1.8544 * (P / d^2)$ , where the applied load P is in kgf, the average dimension d of the indentation marks is in mm, with the resulting hardness number expressed in kgf/mm<sup>2</sup>. Results showed an average Vickers hardness of  $648.4 \pm 107$  (with a range of 208.9) HV 10 gf (corresponding to about 5.5 in the Mohs scale). It is worth noting that the applied load of 10 gf was selected in order to avoid cracking after indentation, and have a proper evaluation of the actual hardness of the investigated material.

Kircherite is non-pleochroic, negative uniaxial with  $\omega = 1.510(2)$  and  $\varepsilon = 1.502(2)$ . The refractive indices were determined by the double variation method (see Su et al. 1987 and references therein) and the grain was oriented with the spindle stage so as to measure the refractive indices (Gunter et al. 2005 and references therein).

According to the various studies done in the last decade on the rare minerals which are typically observed in the cavities of the ejecta of Latium (e.g. Della Ventura et al., 1992, 1993, 1999, Bellatreccia et al., 2002) the mineral formed during late-stage metasomatic processes related to the volcanic activity.

## CHEMICAL COMPOSITION

The composition of kircherite was determined using a JEOL JXA 8200 WD-ED electron microprobe at INGV, Rome. Operating conditions were 15 kV and 4.95 nA, with a beam diameter of 5 µm; counting time was 10 s on both peak and background. Standards, spectral lines, and crystals used were: sodalite (AlK $\alpha$ , TAP; SiK $\alpha$ , PET; NaK $\alpha$ , TAP; ClK $\alpha$ ,



PET) augite (CaK $\alpha$ , PET; MgK $\alpha$ , TAP; FeK $\alpha$ , LIF), orthoclase (KK $\alpha$ , PET), anhydrite (SK $\alpha$ , PET), spessartine (MnK $\alpha$ , LIF), TiO (TiK $\alpha$ , LIF) and fluorite (FK $\alpha$ , TAPH). Data reduction used the ZAF correction method. Analytical errors are 1% relative for major elements and 5% relative for minor elements. The crystal fragment used for single-crystal refinement was found to be homogeneous within analytical error. The chemical composition and empirical formula, calculated on the basis of 216 (Si+Al) atoms per formula unit, are given in Table 1; site populations are based on the structure refinement. The simplified ideal charge-balanced formula is: [Na<sub>90</sub>Ca<sub>36</sub>K<sub>18</sub>] <sub>$\Sigma$ =144</sub>(Si<sub>108</sub>Al<sub>108</sub>O<sub>432</sub>)(SO<sub>4</sub>)<sub>36</sub>·6H<sub>2</sub>O, which can be expressed as {[Na<sub>5</sub>Ca<sub>2</sub>K] <sub>$\Sigma$ =8</sub>(Si<sub>6</sub>Al<sub>6</sub>O<sub>24</sub>)(SO<sub>4</sub>)<sub>2</sub>·0.33H<sub>2</sub>O} × 18. This requires: K<sub>2</sub>O 4.11, Na<sub>2</sub>O 13.51, CaO 9.78, Al<sub>2</sub>O<sub>3</sub> 26.68, SiO<sub>2</sub> 31.44, SO<sub>3</sub> 13.96, H<sub>2</sub>O 0.52, Total 100.00 wt.%. The H<sub>2</sub>O content was calculated and checked on the basis of the single-crystal refinement, assuming that the 'cancrinite cages' host only H<sub>2</sub>O, and that the (SO<sub>4</sub>)<sup>2-</sup> groups missing to reach 36 per unit cell are substituted by (CO<sub>3</sub>)<sup>2-</sup> + (H<sub>2</sub>O) + Cl<sup>-</sup> + F<sup>-</sup> in the 'losod' and 'sodalite cages' (see structure description); FTIR spectroscopy (see below) showed only H<sub>2</sub>O and a small but yet significant amount of CO<sub>2</sub>; no OH was detected.

#### X-RAY DIFFRACTION AND DESCRIPTION OF THE STRUCTURE

The powder X-ray diffraction data of kircherite (Table 2) were collected at the Dipartimento di Scienze Geologiche, Università Roma Tre, with a Scintag X1 diffractometer using: CuK $\alpha$  ( $\lambda$ =1.5418 Å) radiation, fixed divergence slits, and a Peltier-cooled Si(Li) detector (resolution < 200eV). A divergent slit width of 2 mm and a scatter slit width of 4 mm were employed for the beam source; a receiving slit width of 0.5 mm and scatter slit width of 0.2 mm were used for the detector. Data were collected in step-scan mode: 2-60° 2 $\theta$  range, step-size 0.02° 2 $\theta$ , counting time 3 s/step. Silicon powder SRM 640d was used as internal standard. The unit-cell parameters, determined using the least

squares refinement program LSUCRIPC (Garvey 1986), are (in Å):  $a = 12.881(5)$ ,  $c = 95.28(5)$ ,  $V = 13,690(10) \text{ Å}^3$ .

## Structure determination and refinement

A crystal of 0.73x0.40x0.27 mm was used for single crystal X-ray diffraction on a Bruker AXS Smart Apex diffractometer, with  $\text{MoK}\alpha$  ( $\lambda = 0.71073 \text{ Å}$ ) radiation and working at 45 kV and 30 mA, at the Dipartimento di Scienze della Terra e dell'Ambiente, Università di Pavia. The detector-to crystal working distance was 8 cm.  $L_p$  and empirical absorption corrections (SADABS, Sheldrick 1998) were applied. The refined unit-cell parameters were obtained from 9259 reflections with  $I > 10\sigma(I)$  collected in the  $2\theta$  range  $5\text{--}70^\circ$ . Ten data sets of 900 images were collected for 5 seconds performing  $0.2^\circ$   $\omega$ -scans at different  $\phi$  angles ( $0, 90, 180$  and  $270^\circ$  with the detector at  $\theta = 20^\circ$  and  $0, 45, 90, 135, 180$  and  $270^\circ$  with the detector at  $\theta = 50^\circ$ ). Indexing of reflections in images was compatible with a rhombohedral lattice [ $a = 12.8767(7)$ ,  $c = 95.244(6) \text{ Å}$ , in the hexagonal setting]. Integration in the  $2\text{--}30^\circ$   $\theta$ -range yielded 81225 reflections compatible with a maximum  $3m1$  Laue symmetry. The structure was tentatively solved in the space group  $R3$  by direct methods using SIR 2004 (Burla et al. 2005), which supplied an incomplete model with an  $R$ -value of 24.7 %, consisting mainly of framework cations and anions. The structure refinement was completed by adding atoms to the model extracted from Fourier difference maps. This allowed us to find extraframework cations and anionic groups  $(\text{SO}_4)^{2-}$ . We obtained a final model with anisotropic displacement parameters yielding an agreement factor of  $R = 0.125$  for 11517 reflections with  $I > 2\sigma(I)$ , and  $R = 0.135$  for all 13437 unique reflections. There were 12 four-fold coordinated cations composing the framework; and no Si-Al ordering was found. The observed staking sequence in the hexagonal cell, following the Zhdanov notation (Zhdanov, 1945; Patterson and Kasper, 1959), was:

207        - + + + + + + + + + -    - + + + + + + + + + -    - + + + + + + + + + -  
 (A) C A B C A B C A B C A (C) B C A B C A B C A B C (B) A B C A B C A B C A B (A)  
 0 1 2 3 4 5 6 7 8 9 10 11 12 13 14 15 16 17 18 19 20 21 21 23 24 25 26 27 28 29 30 31 32 33 34 35 36

209        ..., where A, B and C represent the position of rings of tetrahedra within layers. The  
 210        sequence for the rhombohedral cell is given below.

211                        - + + + + + + + + + -  
 (A) C A B C A B C A B C A [C]  
                          0 1 2 3 4 5 6 7 8 9 10 11 12

213        Therefore the sequence is expressed as an even period (12) and a different basic partition  
 214        (i.e.,  $3 \times 12 [(10)(2)]$ ), and thus, following Patterson and Kasper (1959), should have a  
 215        rhombohedral lattice. Both successions are centrosymmetric and both centers are in  
 216        spheres. Therefore the space group should be  $R3m$ . However, so far all the cancrinite  
 217        related minerals (but cancrsilite, where the Si:Al is not 1:1) have shown Si-Al ordering  
 218        among the tetrahedral sites, and the  $R3m$  space group would not allow for such ordering.  
 219        Therefore we tried to lower the symmetry to that of space group  $R3$ . This model converged  
 220        to a lower  $R$ -index (0.108). It had 24 four-fold sites this time showing ordering of Al and Si  
 221        in 12 sites, respectively. Testing this model with PLATON/addsym (Spek 2008) yielded a  
 222        higher symmetry model in  $R32$  with 14 fourfold sites in the framework (7 Al + 7 Si sites).  
 223        Refining for the presence of inversion center yielded 0.57(9) of merohedral twinning.  
 224        Refinement of this model produced better <Al-O> and <Si-O> distances and maintained  
 225        the Al and Si ordered. Although we cannot rule out a center of symmetry, the model with  
 226        symmetry  $R3$  showed no ordering; thus, we kept the highest symmetry allowing ordering of  
 227        Al and Si. Refinement converged to  $R = 0.084$  for 8131 reflections with  $I > 2\sigma(I)$ , and  $R =$   
 228        0.088 for all 8908 unique reflections [ $R_{\text{int}} = 0.0308$ , 69 restraints and 515 parameters,  
 229        Goodness of fit on  $F^2 = 1.056$ ]. The framework of tetrahedra builds up a series of cages,  
 230        which are filled by cations and anions/anionic groups. The observed cage topologies are  
 231        'cancrinite cages' ( $\epsilon$ ), [ $4^36^5$ ] in the IUPAC nomenclature (McCusker et al. 2001), [ $4^66^8$ ]

'sodalite cages', and  $[4^6 6^{11}]$  'losod cages'. The extraframework cation positions showed strong static disorder and therefore we chose to refine those as split sites. Displacement parameters of atoms in a split site were constrained to be equal. The model also has 6 anionic groups: 2 out of them (those located at the 'losod cages', see description of the structure) are ordered; four are located in 'sodalite cages' in off-axis positions and were refined with isotropic displacement parameters. Careful search for maxima in the Fourier-difference maps allowed location of some of the oxygen atoms at the vertexes of the  $(\text{SO}_4)^{2-}$  groups. These were added to the model and refined with a soft constraint on the bond-length; in order to let the model to reach a minimum, displacement parameters were constrained to be equal to those observed for the ordered  $(\text{SO}_4)^{2-}$  groups. Final atomic coordinates and equivalent isotropic displacement parameters are given in Table 4, selected distances for framework cations in Table 5a and selected distances for extra-framework cations and anionic groups in Table 5b and 5c (the CIF has been deposited as electronic supplemental material).

#### FTIR SPECTROSCOPY

The powder FTIR spectrum of kircherite was collected at the Dipartimento di Scienze Geologiche, Università Roma Tre on a Nicolet Magna 760 FTIR spectrometer equipped with a DTGS detector and a KBr beamsplitter; the nominal resolution was  $4\text{ cm}^{-1}$  and 64 scans were averaged for each sample and for the background. The spectrum was collected on a KBr disk with about 1 mg of sample in 150 mg of KBr. Single-crystal FTIR spectra were collected on crystal fragments  $\sim 30\text{ }\mu\text{m}$  thick using a NicPlan microscope equipped with a liquid nitrogen-cooled MCT detector; the nominal resolution was  $4\text{ cm}^{-1}$  and 128 scans were averaged for each sample and for the background.

The infrared powder spectrum of kircherite (Fig. 3a) shows a broad absorption from  $3740\text{ cm}^{-1}$  to  $3000\text{ cm}^{-1}$  due to the stretching modes plus the bending overtone ( $\nu_1$ ,  $\nu_3$  and

258  $2\nu_2$ ) of the H<sub>2</sub>O molecule(s) and at 2338 cm<sup>-1</sup> a small but sharp absorption assigned to the  
259 stretching mode ( $\nu_3$ ) of the CO<sub>2</sub> molecules (Della Ventura et al. 2005, 2007, 2008). This  
260 value is in the range observed for CO<sub>2</sub> bearing cancrinite group minerals, where the  
261 wavenumber of this band has been observed to vary from 2338 cm<sup>-1</sup> for fantappièite  
262 (Cámara et al. 2010) up to 2352 cm<sup>-1</sup> for marinellite (Bellatreccia et al. 2007). In the  
263 frequency region from 400 to 1750 cm<sup>-1</sup> (Fig. 3b) there is a broad band due to the bending  
264 mode ( $\nu_2$ ) of the H<sub>2</sub>O molecule at 1635 cm<sup>-1</sup> and a multi-component strong band at 1200-  
265 1000 cm<sup>-1</sup>, which can be assigned to the stretching modes of the (SO<sub>4</sub>)<sup>2-</sup> and TO<sub>4</sub> groups  
266 (Moenke 1974; Ross 1974). A sharp but very weak absorption is observed at 1384 cm<sup>-1</sup>  
267 which can be assigned to (CO<sub>3</sub>)<sup>2-</sup> groups. A group of well-defined bands occur in the range  
268 800-500 cm<sup>-1</sup>; in particular, six absorptions at 698, 651, 609, 590, 546 and a shoulder at  
269 737 cm<sup>-1</sup> are resolved. Finally, a very intense and convoluted absorption is observed at  
270 around 446 cm<sup>-1</sup>. As already discussed in previous papers (e.g., Ballirano et al. 1996a;  
271 Cámara et al. 2005, 2010) this spectral region is characteristic of any cancrinite group  
272 species and is useful for identification purposes. In this particular case, although being  
273 typical of kircherite, it shows some similarities with the spectra of haüyne, franzinite and  
274 fantappièite (Ballirano et al. 1996a; Cámara et al. 2005, 2010).

275 The single-crystal FTIR spectrum was collected in the 6000-650 cm<sup>-1</sup> range; the  
276 4000 to 1500 cm<sup>-1</sup> region is displayed in Figure 5. It shows a very intense multi-component  
277 band which can be resolved into three main components at 3527 cm<sup>-1</sup>, 3412 cm<sup>-1</sup> and  
278 3246 cm<sup>-1</sup> which can be assigned to the stretching modes ( $\nu_1$  and  $\nu_3$ ) and the first bending  
279 overtone ( $2\nu_2$ ) of the H<sub>2</sub>O molecule(s), respectively. The spectrum also shows a very  
280 sharp absorption at 2338 cm<sup>-1</sup> which confirm the presence of CO<sub>2</sub> molecules in the  
281 structural pores of kircherite (Della Ventura et al. 2005, 2007, 2008). The broad absorption  
282 at 2125 cm<sup>-1</sup> can be assigned to the first overtone or combination modes of the T-O bonds  
283 and to the first overtone of the asymmetric stretching mode ( $\nu_3$ ) of the (SO<sub>4</sub>)<sup>2-</sup> group (Della

Ventura et al. 2008). The strong absorption at  $1636\text{ cm}^{-1}$  is due to the  $\text{H}_2\text{O}$  bending mode ( $\nu_2$ ) and the shoulder at  $1687\text{ cm}^{-1}$  can be attributed to combination of T-O modes. Finally, a broad absorption at around  $5234\text{ cm}^{-1}$  (not shown) is assigned to the combination of the stretching ( $\nu_3$ ) + bending ( $\nu_3$ ) modes of  $\text{H}_2\text{O}$  (Ihinger et al. 1994). The absence of bands in the  $4300\text{--}4100\text{ cm}^{-1}$  range (inset in Fig. 5), due to the combination modes of the in OH group (Ihinger et al. 1994), rules out the presence of hydroxyl groups in kircherite.

## DESCRIPTION OF THE CRYSTAL STRUCTURE

The structure has six 'cancrinite cages' ( $\epsilon$ ),  $[4^36^5]$  in the IUPAC nomenclature (McCusker et al. 2001), 24  $[4^66^8]$  'sodalite cages' (S), and 6  $[4^66^{11}]$  'losod cages' (Lo) within the unit cell. There is a unique sequence of cages, and adjacent sequences are shifted  $1/3$  along  $[00.1]$ . Different types of cages are ordered as  $\epsilon\text{SSSLoSSSLoSSS}\epsilon$  (Fig. 6).

### *Cancrinite ( $\epsilon$ ) cages*

Cancrinite cages contain ( $\text{H}_2\text{O}$ ) groups, which coordinate Na atoms at Na1 site in the  $6\text{mR} \perp [00.1]$  window shared by two consecutive  $\epsilon$ -cages and to Ca atoms at the other  $6\text{mR} \perp [00.1]$  windows with long and weak bonds ( $2.93\text{ \AA}$ ). Refined site scattering is compatible with almost full occupancy of  $\text{H}_2\text{O}$  in one on-axis position completing the ditrigonal pyramid corresponding to the Na coordinating environment. There are 6  $\epsilon$  cages per unit cell, which accounts for 6  $\text{H}_2\text{O}$  p.f.u.

### *Losod cages*

Six  $[4^66^{11}]$  cages (losod cages) are present p.f.u., which match with two sodalite cages ( $[4^66^8]$ ) along  $[00.1]$ . The losod cage occurs in many members of the group: bystrite and carbobystrite, liottite (Ballirano et al. 1996b), franzinite, tounkite, biachellaite, fantappi  ite, sacrofanite, and obviously kircherite. In kircherite, each losod cage contains

two  $(\text{SO}_4)^{2-}$  groups ordered with apexes pointing oppositely along  $[00.1]$ , which coordinate 3 K atoms off-axis in the plane between the bases of the two  $(\text{SO}_4)^{2-}$  groups, Ca atoms at the Ca3 site in one of the  $6\text{mR} \perp [00.1]$  windows and Ca and minor Na atoms at the Ca7 site centered approximately at the other the  $6\text{mR} \perp [00.1]$  window. Na and Ca at the Na2 and Na4 sites in the center of the six membered rings in the wall of the cage (hereafter  $6\text{mR} \parallel [00.1]$ ) also coordinates with the oxygen apexes of the  $[(\text{S1})\text{O}_4]^{2-}$  and  $[(\text{S2})\text{O}_4]^{2-}$  anionic groups, respectively. These two cation positions have different occupancy as a function of the anion located at the center of the adjacent sodalite cages.

#### *Sodalite cages*

Sodalite cages ( $[4^6 6^8]$ ) are the most frequent cages in kircherite (up to 24 sodalite cages per unit cell). They mostly contain  $(\text{SO}_4)^{2-}$  groups disordered so that it was not possible to find the position of all oxygen atoms in the four symmetrically independent sites. This disorder is common in all the minerals of the cancrinite group showing this type of cage, usually containing sulfate groups in more than one orientation, as well as split cation sites in the two  $6\text{mR} \perp [00.1]$  and the six  $6\text{mR} \parallel [00.1]$  windows that may host Na or Ca cations. Sodalite cages also contain minor Cl (and F) that coordinates Ca and  $(\text{H}_2\text{O})$  which coordinates Na (up to complete 36 anion groups and anions per formula unit; see Table 6). Therefore the composition of sodalite cages are mostly related to haüynic and to a lesser degree sodalitic and noseanic. The white color of kircherite probably excludes the presence of  $(\text{S}_3)^-$  at the sodalitic cages, which usually results in the blue coloration of these minerals (Ostroumov et al. 2002; Fleet et al. 2005). Overall, the number and type of cages in the unit cell account for a maximum of 36  $(\text{SO}_4)^{2-}$  groups and 6  $(\text{H}_2\text{O})$  molecules (or  $\text{Cl}^-$  anions).

#### *Site assignment*

Assigned site population on the basis of observed site scattering and site geometry (i.e., bonding environment) is reported Table 6. There is a slight disagreement between

the Ca + K assignments based on the refinement as compared to that determined by electron microprobe. However, considering the similar scattering power of both atomic species, the observed disagreement might be ascribed to erroneous assignment of elements to these sites, which is done on the basis of the mean bond lengths, as the bonding environments put some restrictions to the occupying species on the basis of their ionic radii. Considering the large cell, the complexity of the structure and the observed *R*-factor, the disagreement should be ascribed to difficulties on refining the split positions thus leading to local geometries incompatible for Ca population or excess observed site scattering. Disagreement with the calculated site scattering for cation sites from EMP analyses is 7.8%. This is the case in particular for the split sites K6B, K9B, K1G and K1L, which account for 17.53 K apfu; their bonding environment is too large for Ca and Na.

Considering the extraframework composition obtained by EMP analyses and the dominant anionic species or groups in the cages, the simplified ideal charge-balanced formula is:  $[\text{Na}_{90}\text{Ca}_{36}\text{K}_{18}]_{\Sigma=144}(\text{Si}_{108}\text{Al}_{108}\text{O}_{432})(\text{SO}_4)_{36} \cdot 6\text{H}_2\text{O}$ , which can be expressed as  $\{[\text{Na}_5\text{Ca}_2\text{K}]_{\Sigma=8}(\text{Si}_6\text{Al}_6\text{O}_{24})(\text{SO}_4)_2 \cdot 0.33\text{H}_2\text{O}\}^*18$ . This requires: K<sub>2</sub>O 4.11, Na<sub>2</sub>O 13.51, CaO 9.78, Al<sub>2</sub>O<sub>3</sub> 26.68, SiO<sub>2</sub> 31.44, SO<sub>3</sub> 13.96, H<sub>2</sub>O 0.52, Total 100.00 wt.%.

The compatibility indices (Mandarino 1981) are:  $(1 - K_P)/K_C = -0.022$  (i.e., excellent) by using  $D_{\text{calc}}$ , and  $(1 - K_P)/K_C = -0.038$  (i.e., excellent) by using  $D_{\text{meas}}$ , indicating excellent agreement between physical and chemical data.

#### RELATION TO OTHER SPECIES

Kircherite is a new mineral of the cancrinite-sodalite group and is a member of the subgroup with a complex sequence. Within this subgroup, kircherite, having 36 layers (in the hexagonal setting; 12 in the rhombohedral), is the cancrinite with the longest complex sequence described to date. Considering the rhombohedral setting, it is the third mineral of the cancrinite-sodalite group showing 12 layers sequence, along with tounkite (Rozenberg



et al. 2004) and marinelite (Bonaccorsi and Orlandi 2003). The three structures have very different layers sequences, Zhdanov symbol and number and type of cages:

Marinelite:	ABCBCBACBCBC	1(4)1 1(4)1	2 lio, 4 sod, 6 $\epsilon$
Tounkite:	ABABACACABAC	(2)211(2)211	2 lio, 2 sod, 8 $\epsilon$
Kircherite:	ACABCABCABCA	[(10)(2)]	2 los, 8 sod, 2 $\epsilon$

being lio = 'liottite cages' [ $4^6 6^{17}$ ]. The different topology in terms of cages constrain the chemistry of the three different minerals. Nevertheless, a correct identification cannot be done on the basis of only a chemical analysis, and requires a X-ray diffraction.

Careful inspection of the sequence (Fig. 6) reveals that the structure of kircherite can be derived from that of sodalite by inserting a shifted layer every 11 layers, as for fantappièite and franzinite. In the case of fantappièite the structure can be obtained from sodalite by inserting a shifted layer every 10 layers [sequence (9)(2)], and from franzinite by inserting a shifted layer every 9 layers [sequence (8)(2)]. Therefore, kircherite represents the third member of a particular subgroup in which ordered interstratified sodalite-cancrinite sequences are found to follow the scheme: (*nsod*)(*can*), for  $n = 1, 2, 3, 4, \dots$ . Expected sequences are (3)(2), (4)(2), (5)(2), (6)(2), (7)(2), (8)(2), (9)(2), (10)(2), ..., of which the last three have been discovered. Two of these have hexagonal cells [i.e., (5)(2) and (8)(2)], while the remainder have rhombohedral cells and therefore sequences of 15, 18, 24, 27, 33 and 36 layers in the hexagonal setting, corresponding to *c* axis lengths of *ca* 39.7, 47.6, 63.5, 71.4, 87.3, and 95.2 Å.

#### ACKNOWLEDGEMENTS

Thanks are due to late Mr. Luigi Mattei who provided us with the sample allowing the discovery of this new mineral. Roberto Gastoni CNR-IGG of Pavia (Italy) assisted with sample preparation for EMPA. FC thanks the Dipartimento di Scienze della Terra e dell'Ambiente, Università di Pavia (Italy) and CNR-IGG of Pavia (Italy) for granting access

387 to the single-crystal diffractometer. The suggestions of two anonymous reviewers and  
388 Associate Editor Fernando Colombo helped to improve the quality of the manuscript.  
389

## REFERENCES

- ASTM Standard E384 08ae1 (2008) Standard Test Method for Microindentation Hardness of Materials. ASTM International, West Conshohocken, PA, DOI: 10.1520/E0384-08AE01, [www.astm.org](http://www.astm.org).
- Ballirano, P., Maras, A., and Buseck, P.R. (1996a) Crystal chemistry and IR spectroscopy of  $\text{Cl}^-$  and  $\text{SO}_4^{2-}$  bearing cancrinite-like minerals. *American Mineralogist*, 81, 1003-1012.
- Ballirano, P., Merlino, S., Bonaccorsi, E., and Maras, A. (1996b) The crystal structure of liottite, a six-layer member of the cancrinite group. *Canadian Mineralogist*, 34, 1021-1030.
- Ballirano, P., Bonaccorsi, E., Maras, A., and Buseck, P.R. (1997) The crystal structure of afghanite, the eight-layer member of the cancrinite group: evidence for long-range Si, Al ordering. *European Journal of Mineralogy*, 9, 21-30.
- Bellatreccia, F., Della Ventura, G., Williams, T.C., Lumpkin, G.R., Smith, K.L., and Colella, M. (2002) Non-metamict zirconolite polytypes from the feldspathoid-bearing alkali-syenitic ejecta of the Vico volcanic complex (Latium, Italy). *European Journal of Mineralogy*, 14, 809-820.
- Bellatreccia, F., Della Ventura, G., Parodi, G.C., Pucci, R., and Mattei, L. (2007) New data on marinellite, a mineral of the cancrinite-sodalite group. *Geoitalia 2007*. Sesto Forum Italiano di Scienze della Terra. Rimini, 12-14 settembre 2007, Epitome, 1050.
- Bonaccorsi, E. and Merlino, S. (2005) Modular microporous minerals: cancrinite-davyne group and CSH phases. In G. Ferraris and S. Merlino (Eds.), *Micro and mesoporous mineral phases*, p. 241-290. *Reviews in Mineralogy and Geochemistry*, Mineralogical Society of America and the Geochemical Society, Washington, D.C.

415 Bonaccorsi, E. and Orlandi, P. (2003) Marinellite, a new feldspatoid of the cancrinite-  
 416 sodalite group. *European Journal of Mineralogy*, 15, 1019-1027.

417 Bonaccorsi, E., Ballirano, P., and Cámara F. (2012) The crystal structure of sacrofanite,  
 418 the 74 Å phase of the cancrinite-sodalite supergroup. *Microporous & Mesoporous*  
 419 *Materials*, 147, 318-326.

420 Burla, M.C., Caliendo, R., Camalli, M., Carrozzini, B., Cascarano, G.L., De Caro, L.,  
 421 Giacobazzo, C., Polidoria, G., and Spagna, R. (2005) SIR2004: an improved tool for  
 422 crystal structure determination and refinement. *Journal of Applied Crystallography*,  
 423 38, 381-388.

424 Cámara, F., Bellatreccia, F., Della Ventura, G., and Mottana, A. (2005) Farneseite, a new  
 425 mineral of the cancrinite - sodalite group with a 14-layer stacking sequence:  
 426 occurrence and crystal structure. *European Journal of Mineralogy*, 17, 839-846.

427 Cámara, F., Bellatreccia, F., Della Ventura, G., Mottana, A., Bindi, L., Gunter, M.E., and  
 428 Sebastiani, M. (2010) Fantappièite, a new mineral of the cancrinite - sodalite group  
 429 with a 33-layer stacking sequence: occurrence and crystal structure. *American*  
 430 *Mineralogist*, 95, 472-480.

431 Chukanov, N.V., Rastsvetaeva, R.K., Pekov, I.V., and Zadov, A.E. (2007) Alloriite,  
 432  $\text{Na}_5\text{K}_{1.5}\text{Ca}(\text{Si}_6\text{Al}_6\text{O}_{24})(\text{SO}_4)(\text{OH})_{0.5} \cdot \text{H}_2\text{O}$ , a new mineral species of the cancrinite  
 433 group. *Geology of Ore Deposits*, 49, 752–757.

434 Chukanov, N.V., Rastsvetaeva, R.K., Pekov, I.V., Zadov, A.E., Allori, R., Zubkova, N.V.,  
 435 Giester, G., Pushcharovsky, Yu, D., and Van, K.V. (2008) Biachellaite  
 436  $(\text{Na,Ca,K})_8(\text{Si}_6\text{Al}_6\text{O}_{24})(\text{SO}_4)_2(\text{OH})_{0.5} \cdot \text{H}_2\text{O}$ , a new mineral of the cancrinite group.  
 437 *Proceedings of the Russian Mineralogical Society*, 137(3), 57–66 (Russian with  
 438 English abstract).

439 Della Ventura, G., Di Lisa, A., Marcelli, M., Mottana, A., and Paris, E. (1992) Composition  
 440 and structural state of alkali feldspars from ejecta in the Roman potassic province,  
 441 Italy; petrological implications. *European Journal of Mineralogy*, 4, 411-424.

442 Della Ventura, G., Parodi, G.C., Mottana A., and Chaussidon, M. (1993) Pepprossiite (Ce),  
 443 a new mineral from Campagnano (Italy): the first anhydrous rare-earth-element  
 444 borate. *European Journal of Mineralogy*, 5, 53-58.

445 Della Ventura, G., Williams, T.C., Cabella, R., Oberti, R., Caprilli, E., and Bellatreccia, F.  
 446 (1999) Britholite - hellandite intergrowths and associated REE-minerals from the  
 447 alkali-syenitic ejecta of the Vico volcanic complex (Latium, Italy): petrological  
 448 implications bearing on REE mobility in volcanic systems. *European Journal of*  
 449 *Mineralogy*, 11, 843-854.

450 Della Ventura, G., Bellatreccia, F., and Bonaccorsi, E. (2005) CO<sub>2</sub> in minerals of the  
 451 cancrinite-sodalite group: pitiglianoite. *European Journal of Mineralogy*, 17, 847-  
 452 851.

453 Della Ventura, G., Bellatreccia, F., Parodi, G.C., Cámara, F., and Piccinini, M. (2007)  
 454 Single-crystal FTIR and X-ray study of vishnevite, ideally  
 455 [Na<sub>6</sub>(SO<sub>4</sub>)] [Na<sub>2</sub>(H<sub>2</sub>O)<sub>2</sub>](Si<sub>6</sub>Al<sub>6</sub>O<sub>24</sub>). *American Mineralogist*, 92, 713-721.

456 Della Ventura, G., Bellatreccia, F., and Piccinini, M. (2008) Channel CO<sub>2</sub> in feldspathoids:  
 457 new data and new perspectives. *Rendiconti Lincei* 19, 141-159.

458 De Rita D., Funiciello R., Rossi U., and Sposato A. (1983) Structure and evolution of the  
 459 Sacrofano-Baccano caldera, Sabatini volcanic complex, Rome. *Journal of*  
 460 *Volcanology and Geothermal Research*, 17, 219-236.

461 De Rita D., Funiciello R., Corda L., Sposato A., and Rossi U. (1993) Volcanic Units. In:  
 462 Sabatini Volcanic Complex (Ed. M. Di Filippo). Quaderni de "La ricerca scientifica",  
 463 114, Progetto Finalizzato "Geodinamica", monografie finali, 11: 33-79.

464 Fleet, M. E., Liu, X., Harmer, S. L., and Nesbitt, H.W. (2005) Chemical state of sulfur in  
 465 natural and synthetic lazurite by S K-edge Xanes and X-ray photoelectron  
 466 spectroscopy. *Canadian Mineralogist*, 43, 1589-1603.

467 Garvey R.G. (1986) LSUCRIPC, least squares unit-cell refinement with indexing on the  
 468 personal computer. *Powder Diffraction* 1, 89.

469 Gunter, M.E., Downs, R.T., Bartelmehs, K.L., Evans, S.H., Pommier, C.J.S., Grow, J.S.,  
 470 Sanchez, M.S., and Bloss, F.D. (2005) Optic properties of centimeter-sized crystals  
 471 determined in air with the spindle stage using EXCALIBRW. *American Mineralogist*,  
 472 90, 1648-1654.

473 Ihinger, P.D., Hervig, R.L., and McMillan. P.F. (1994) Analytical methods for volatiles in  
 474 glasses. In M.R. Carroll and J.R. Holloway, Eds., *Volatiles in Magmas*, p. 67-121.  
 475 Reviews in Mineralogy, Mineralogical Society of America, Washington, D.C.

476 Khomyakov, A.P., Cámara, F., and Sokolova, E. (2010) Carbobystrite,  
 477  $\text{Na}_8[\text{Al}_6\text{Si}_6\text{O}_{24}](\text{CO}_3) \cdot 4\text{H}_2\text{O}$ , a new cancrinite-group mineral species from the Khibina  
 478 alkaline massif, Kola peninsula, Russia: description and crystal structure. *Canadian*  
 479 *Mineralogist*, 48, 291-300.

480 Mandarino, J.A. (1981) The Gladstone-Dale relationship: Part IV. The compatibility  
 481 concept and its application. *Canadian Mineralogist*, 19, 441-450

482 McCusker, L.B., Liebau, F., and Engelhardt, G. (2001) Nomenclature of structural and  
 483 compositional characteristics of ordered microporous and mesoporous materials  
 484 with inorganic hosts. *Pure Applied Chemistry*, 73, 381-394.

485 Moenke, H.H.W. (1974) Silica, the three-dimensional silicates, borosilicates and beryllium  
 486 silicates. In V.C. Farmer (Ed.), *The infrared spectra of Minerals*, 365-382. The  
 487 Mineralogical Society, London.

488 Ostroumov, M., Fritsch, E., Faulques, E., and Chauver, O. (2002) Etude spectrometrique  
 489 de la lazurite du Pamir, Tajikistan. *Canadian Mineralogist*, 40, 885-893.

490 Patterson, A.L. and Kasper, J.S. (1959) Close packing. *In* International Tables for X-ray  
 491 Crystallography, Vol II, The Kynoch Press, Birmingham, 342-354.  
 492 Rastsvetaeva, R.K. and Chukanov, N.V. (2008) Model of the crystal structure of  
 493 biachellaite as a new 30-layer member of the cancrinite group. *Crystallography*  
 494 *Reports*, 53, 981-988.  
 495 Rastsvetaeva, R.K., Ivanova, A.G., Chukanov, N.V., and Verin, I.A. (2007): Crystal  
 496 structure of alloriite. *Doklady Earth Sciences*, 415, 815–819.  
 497 Rinaldi, R. and Wenk, H.R. (1979) Stacking variations in cancrinite minerals. *Acta*  
 498 *Crystallographica*, A35, 825-828.  
 499 Ross, S.D. (1974) Sulphates and other oxy-anions of Group VI. In V.C. Farmer (Ed.), *The*  
 500 *infrared spectra of Minerals*, 423-444. The Mineralogical Society, London.  
 501 Rozenberg, K.A, Sapozhnikov, A.N., Rastsvetaeva, R.K., Bolotina, N.B., and Kashaev,  
 502 A.A. (2004) Crystal structure of a new representative of the cancrinite group with a  
 503 12-layer stacking sequence of tetrahedral rings. *Crystallography Reports*, 49, 635-  
 504 642.  
 505 Sheldrick, G.M. (1998) SADABS. Bruker AXS Inc., Madison, Wisconsin, USA.  
 506 Spek, A.L. (2008) PLATON, A Multipurpose Crystallographic Tool, Utrecht University,  
 507 Utrecht, The Netherlands.  
 508 Su, S.C., Bloss, F.D., and Gunter, M.E. (1987) Procedures and computer programs to  
 509 refine the double variation method. *American Mineralogist*, 72, 1011-1013.  
 510 Zhdanov, G.S. (1945) The numerical symbol of close packing of spheres and its  
 511 application in the theory of close packings. *Comptes rendus de l'Académie des*  
 512 *Sciences de l'Union des Républiques Soviétiques Socialistes*, 48, 39-42.

## TABLE CAPTIONS

**Table 1.** Chemical composition determined using electron microprobe (mean of 18 analyses) and empirical formula of kircherite calculated on the basis of  $\Sigma(\text{Si}+\text{Al}) = 216$  apfu.

**Table 2.** Powder X-ray diffraction data for kircherite.

**Table 3.** Crystal data and structure refinement for kircherite.

**Table 4.** Atomic coordinates and equivalent isotropic displacement parameters ( $\text{\AA}^2$ ) for framework cations and anions in kircherite.

**Table 4 ctd.** Atomic coordinates and equivalent isotropic displacement parameters ( $\text{\AA}^2$ ) for extraframework cations and anions in kircherite.

**Table 5a.** Selected distances of framework cations for kircherite.

**Table 5b.** Selected distances of extra-framework cations sites for kircherite.

**Table 5c.** Selected distances of extra-framework anionic groups for kircherite.

**Table 6.** Cation site assignments on the basis of observed site scattering and geometries of the sites reported in Table 5 for kircherite



**FIGURE CAPTIONS**

**Fig. 1.** Photomicrographs (crossed polars) of kircherite in thin section: a) kircherite (kir) with k-feldspar (Kf) and biotite (bio); b) typically twinned crystals of kircherite.

**Fig. 2.** a) Photomicrographs and b) morphological sketch of kircherite (sample and photo L. Mattei).

**Fig. 3.** FTIR powder spectrum of kircherite: a) H<sub>2</sub>O (stretching) and CO<sub>2</sub> absorptions (\* = grease); b) low frequency region with the H<sub>2</sub>O (bending), SO<sub>4</sub><sup>2-</sup>, trace of CO<sub>3</sub><sup>2-</sup> and the typical (Si,Al)O<sub>4</sub> absorptions (see text for explanations).

**Fig. 4.** The FTIR powder spectrum of kircherite compared to the spectra of haüyne, franzinite, and fantappièite.

**Fig. 5.** The single-crystal unpolarized-light FTIR spectrum of kircherite; NIR region in the inset.

**Fig. 6.** Projection of the kircherite structure along  $[112; \bar{0}]$  showing the stacking sequence of cages along  $[00.1]$  at  $(0,0,z)$ .  $\epsilon$ : 'cancrinite cage' (gray); s: 'sodalite cage' (light gray); los: 'losod cage' (dark gray). Si: dark gray spheres; Al: light gray spheres.

**Table 1.** Chemical composition determined using electron microprobe (mean of 18 analyses) and empirical formula of kircherite calculated on the basis of  $\Sigma(\text{Si}+\text{Al}) = 216$  apfu.

	Wt. %	Range		apfu
SiO <sub>2</sub>	32.05	31.17-33.31	Si	108.13
Al <sub>2</sub> O <sub>3</sub>	27.13	26.66-27.62	Al	107.87
FeO	0.07	0.00-0.18	$\Sigma$	216.00
K <sub>2</sub> O	4.38	4.15-4.62		
CaO	8.75	8.48-9.29	Ca	31.63
Na <sub>2</sub> O	13.62	12.66-14.02	Fe <sup>2+</sup>	0.20
MgO	0.01	0.00-0.05	K	18.85
MnO	0.02	0.00-0.08	Na	89.09
TiO <sub>2</sub>	0.01	0.00-0.05	Ti	0.03
SO <sub>3</sub>	12.87	12.61-13.46	Mg	0.05
Cl	0.35	0.28-0.42	Mn	0.06
F	0.05	0.00-0.20	$\Sigma$	139.91
H <sub>2</sub> O <sup>‡</sup>	0.61	0.74-0.44		
	99.92	98.75-102.02	SO <sub>4</sub> <sup>2-</sup>	32.58
O=F,Cl	0.10	0.06-0.16	Cl <sup>-</sup>	2.00
Total	99.82	98.65-101.86	F <sup>-</sup>	0.53
			H <sub>2</sub> O <sup>‡</sup>	6.86
			O	430.19

<sup>‡</sup> Calculated on the basis of the single-crystal refinement (see text).

First revision 20/03/2012

**Table 2.** Powder X-ray diffraction data for kircherite.

$I/I_0$ (%)	$d_{meas}$ (Å)	$d_{calc}$ (Å)	$hkl$	$I/I_0$ (%)	$d_{meas}$ (Å)	$d_{calc}$ (Å)	$hkl$
4	31.75	31.76	003	12	2.914	2.914	3,1,11
3	15.88	15.88	006	7	2.886	2.887	0,0,33
10	11.10	11.08	101	2	2.843	2.849	1,1,30; 1,3,13
5	10.85	10.86	012	5	2.817	2.817	3,1,14
15	10.04	10.10	104	4	2.783	2.784	042; 401
2	9.461	9.627	015	4	2.766	2.766	1,2,26; 045
3	6.868	6.842	0,1,11	3	2.751	2.751	2,2,18; 1, 3, 16
17	6.440	6.440	110	100	2.648	2.648	2,1,28; 0,0,36
11	5.809	5.810	0,1,14	3	2.603	2.606	4,0,13
4	5.576	5.568	021	7	2.577	2.581	0,4,14
2	5.460	5.431	024	3	2.549	2.545	324; 235
3	5.292	5.293	0,0,18	3	2.516	2.515	327; 1,0,37
3	5.248	5.253	1,0,16	2	2.499	2.501	2,2,24; 0,4,17
2	5.075	5.051	208	3	2.466	2.472	3,2,10
3	5.012	5.008	0,1,17	5	2.451	2.448	1,1,36; 2,0,35
6	4.792	4.814	0,2,10	5	2.434	2.434	410; 1,2,32
3	4.697	4.689	2,0,11	3	2.408	2.407	0,4,20; 416
3	4.572	4.574	1,0,19	3	2.401	2.402	1,3,25; 2,3,14
3	4.421	4.439	0,2,13	2	2.352	2.351	3,2,16
3	4.329	4.314	2,0,14	6	2.250	2.251	4,0,25; 3,1,29
7	4.215	4.212	211; 122	7	2.168	2.172	0,5,10; 1,0,43
3	4.157	4.152	214	17	2.156	2.157	4,0,28
7	4.107	4.117	125	21	2.147	2.145	3,1,32
7	4.090	4.089	1,1,18	12	2.141	2.140	1,1,42; 333
4	4.070	4.071	0,2,16	3	2.045	2.045	2,2,36; 3,1,35
6	4.037	4.037	1,0,22	3	2.040	2.042	3,0,39; 0,5,19
3	3.983	3.975	128	3	2.003	2.003	511; 152; 4,1,27
3	3.945	3.954	2,0,17	2	1.954	1.952	1,5,11; 0,4,35
52	3.799	3.791	1,2,11	4	1.926	1.926	1,2,44; 4,2,20; 0,5,25
100	3.717	3.718	300	18	1.916	1.916	1,0,49
3	3.657	3.655	2,1,13	3	1.878	1.878	0,1,50
53	3.604	3.607	1,0,25	3	1.873	1.868	0,0,51
60	3.584	3.584	1,2,14	3	1.865	1.866	0,5,28; 2,3,35
24	3.551	3.529	0,0,27	3	1.834	1.834	431; 3,3,27
5	3.466	3.482	0,1,26	3	1.830	1.831	609; 434
5	3.445	3.441	2,1,16	3	1.825	1.825	345; 5,1,22
8	3.370	3.369	1,2,17	2	1.818	1.817	437; 3,2,37
9	3.353	3.367	3,0,12	6	1.796	1.794	1,1,51; 3,4,11
19	3.313	3.326	2,0,23	7	1.793	1.792	2,4,28; 4,1,36
13	3.252	3.255	1,0,28	5	1.787	1.786	520; 5,0,32
65	3.232	3.227	2,1,19	3	1.646	1.646	1,3,49; 6,0,27
38	3.220	3.220	220	11	1.633	1.631	2,4,37; 5,1,34
11	3.152	3.152	0,1,29; 0,2,25	3	1.614	1.614	4,3,28; 1,5,35
9	3.050	3.043	3,0,18	8	1.610	1.610	440; 3,2,46
8	3.021	3.021	2,1,22	4	1.606	1.605	6,0,30; 2,1,55
6	2.994	2.995	318	2	1.573	1.572	0,5,43; 7,0,10
5	2.944	2.943	1,3,10	3	1.568	1.567	0,7,11; 1,5,38

**Table 3.** Crystal data and structure refinement for kircherite.

Temperature	293(2) K	
Wavelength	0.71073 Å	
Crystal system	Trigonal	
Space group	<i>R</i> 32	
Unit cell dimensions	<i>a</i> = 12.8770(7) Å	$\alpha = 90^\circ$
	<i>b</i> = 12.8770(7) Å	$\beta = 90^\circ$
	<i>c</i> = 95.244(6) Å	$\gamma = 120^\circ$
Volume	13677.2(13) Å <sup>3</sup>	
<i>Z</i>	1	
Density (calculated)	2.383 Mg/m <sup>3</sup>	
Crystal size	0.73 x 0.40 x 0.27 mm <sup>3</sup>	
Theta range for data collection	1.28 to 30.03°.	
Index ranges	-18 ≤ <i>h</i> ≤ 17, -18 ≤ <i>k</i> ≤ 18, -133 ≤ <i>l</i> ≤ 133	
Reflections collected	81125	
Independent reflections	8900 [ <i>R</i> <sub>(int)</sub> = 0.0308]	
Completeness to theta = 30.03°	99.7 %	
Refinement method	Full-matrix least-squares on <i>F</i> <sup>2</sup>	
Data / restraints / parameters	8900 / 10 / 510	
Goodness-of-fit on <i>F</i> <sup>2</sup>	1.038	
Final <i>R</i> indices [ <i>I</i> > 2σ( <i>I</i> )]	<i>R</i> 1 = 0.0847, <i>wR</i> <sup>2</sup> = 0.2304	
<i>R</i> indices (all data)	<i>R</i> 1 = 0.0893, <i>wR</i> <sup>2</sup> = 0.2370	
Absolute structure parameter	0.53(9)	
Largest diff. peak and hole	3.246 and -2.136 e.Å <sup>-3</sup>	

**Table 4.** Atomic coordinates and equivalent isotropic displacement parameters ( $\text{\AA}^2$ ) for framework cations and anions in kircherite.

Atom	Wyck.	<i>x/a</i>	<i>y/b</i>	<i>z/c</i>	U(eq)
Si1	9d	0.25209(13)	0	0	0.0153(4)
Si2	18f	0.92141(11)	0.58468(10)	0.028745(16)	0.0138(3)
Si3	18f	0.25017(11)	-0.00038(10)	0.056598(17)	0.0153(3)
Si4	18f	0.33285(11)	0.41471(13)	0.084480(16)	0.0165(3)
Si5	18f	0.41674(13)	0.08479(13)	0.112132(17)	0.0176(3)
Si6	18f	0.24895(14)	0.24891(14)	0.139370(16)	0.0180(3)
Si7	9e	1/3	0.91414(17)	1/6	0.0189(4)
Al1	9d	0	0.74422(14)	0	0.0150(4)
Al2	18f	0.40708(12)	0.08485(12)	0.028747(18)	0.0155(3)
Al3	18f	0.25229(13)	0.25532(13)	0.056187(18)	0.0151(3)
Al4	18f	0.33367(13)	0.91923(15)	0.084777(19)	0.0184(4)
Al5	18f	0.41672(15)	0.33299(12)	0.111910(18)	0.0179(4)
Al6	18f	0.24778(16)	-0.00033(13)	0.139511(19)	0.0206(4)
Al7	9e	0.58118(19)	0.91451(19)	1/6	0.0189(5)
O1	18f	0.1218(4)	0.8853(4)	0.00247(3)	0.0257(6)
O2	18f	0.3374(3)	0.0159(4)	0.01327(4)	0.0216(8)
O3	18f	0.9782(4)	0.6459(4)	0.01398(4)	0.0265(10)
O4	18f	0.7830(3)	0.5489(3)	0.03041(3)	0.0241(6)
O5	18f	0.5400(4)	0.0786(3)	0.02974(3)	0.0273(6)
O6	18f	0.0006(4)	0.6698(5)	0.04121(5)	0.0293(10)
O7	18f	0.3192(4)	-0.0016(4)	0.04249(5)	0.0270(9)
O8	18f	0.1132(4)	0.8975(4)	0.05576(3)	0.0284(6)
O9	18f	0.2539(3)	0.1258(4)	0.05938(3)	0.0286(6)
O10	18f	0.3256(5)	0.9846(4)	0.06921(5)	0.0336(11)
O11	18f	0.3276(5)	0.3547(5)	0.06976(6)	0.0379(11)
O12	18f	0.4495(4)	0.8905(3)	0.08400(4)	0.0354(7)
O13	18f	0.2192(4)	0.4260(4)	0.08817(4)	0.0368(8)
O14	18f	0.3496(6)	0.3371(5)	0.09634(6)	0.0413(12)
O15	18f	0.3505(6)	0.0155(7)	0.09803(7)	0.0561(18)
O16	18f	0.4517(5)	0.2220(5)	0.11056(5)	0.0530(11)
O17	18f	0.5372(6)	0.0802(5)	0.11528(5)	0.0554(12)
O18	18f	0.3335(8)	0.0189(7)	0.12516(8)	0.077(3)
O19	18f	0.3153(7)	0.3075(7)	0.12514(7)	0.0612(19)
O20	18f	0.1171(5)	0.2216(6)	0.13723(5)	0.0691(17)
O21	18f	0.2402(6)	0.1267(6)	0.14278(6)	0.0774(19)
O22	18f	0.6607(9)	0.9789(8)	0.15169(8)	0.086(3)
O23	18f	0.3132(7)	0.9767(7)	0.15362(8)	0.088(3)
O24	18f	0.4455(6)	0.8978(7)	0.16380(6)	0.093(2)

**Table 4 ctd.** Atomic coordinates and equivalent isotropic displacement parameters ( $\text{\AA}^2$ ) for extraframework cations and anions in kircherite.

Atom	Wyck.	Occ.	x	y	z	U(eq)
K1	18f	1	0.21935(14)	0.78244(14)	0.026734(9)	0.0316(2)
Na1	3a	1	0	0	0	0.0620(19)
Na2A	9d	0.616(16)	0	0.49632(18)	0	0.0281(7)
Ca2B	9d	0.384(16)	0	0.49632(18)	0	0.0281(7)
Ca3	6c	1.009(8)	2/3	1/3	0.035016(17)	0.0283(5)
Na4A	18f	0.771(12)	0.4865(2)	0.97775(17)	0.055175(17)	0.0383(6)
Ca4B	18f	0.229(12)	0.4865(2)	0.97775(17)	0.055175(17)	0.0383(6)
Na5A	6c	0.720(14)	0	0	0.06575(15)	0.051(2)
Ca5B	6c	0.280(14)	0	0	0.05922(19)	0.051(2)
Na6A	18f	0.644(9)	0.3399(6)	0.1714(5)	0.08322(4)	0.0451(10)
K6B	18f	0.249(4)	0.4289(6)	0.2173(6)	0.07941(5)	0.0451(10)
Na6B	18f	0.193(8)	0.2762(19)	0.1439(16)	0.08739(14)	0.0451(10)
Na7A	6c	0.05(2)	1/3	2/3	0.08904(2)	0.0354(7)
Ca7B	6c	0.95(2)	1/3	2/3	0.08904(2)	0.0354(7)
Na8A	6c	0.452(15)	2/3	1/3	0.10234(13)	0.055(3)
Na8B	6c	0.08(2)	2/3	1/3	0.1135	0.055(3)
Na8C	6c	0.68(2)	2/3	1/3	0.12063(11)	0.055(3)
K9A	18f	0.236(5)	0.1242(10)	0.2467(9)	0.10791(7)	0.0544(14)
Na9A	18f	0.630(9)	0.1591(7)	0.3183(7)	0.11131(5)	0.0544(14)
Na9B	18f	0.203(7)	0.2035(18)	0.4025(18)	0.11546(13)	0.0544(14)
Na1C	6c	0.53(2)	0	0	0.13014(15)	0.065(4)
Na1D	6c	0.18(3)	0	0	0.1396	0.065(4)
Na1E	6c	0.50(2)	0	0	0.14781(19)	0.065(4)
Na1F	18f	0.23(3)	0.4939(10)	0.9927(7)	0.13870(8)	0.016(3)
K1G	18f	0.411(16)	0.4686(13)	0.930(2)	0.13597(9)	0.117(7)
Na1G	18f	0.367(13)	0.5223	1.0488(18)	0.1413	0.117(7)
Na1K	6c	0.516(17)	1/3	2/3	0.15719(9)	0.044(3)
K1L	18f	0.210(4)	0.2474(9)	0.1287(10)	0.17056(6)	0.0575(16)
Na1L	9d	0.580(7)	1/3	0.1667(9)	1/6	0.0575(16)
Ow25	6c	0.94(4)	0	0	0.02844(18)	0.148(10)
S1	6c	1	0.3333	0.6667	0.00351(2)	0.0270(3)
O1SA	6c	1	0.6667	0.3333	0.01182(7)	0.0530(18)
O1SB	18f	1	0.2093(3)	0.6027(5)	0.00861(5)	0.0464(9)
S2	6c	1	0.3333	0.6667	0.05032(2)	0.0313(4)
O2SA	6c	1	0.3333	0.6667	0.06586(9)	0.0553(8)
O2SB	18f	1	0.2101(4)	0.6033(6)	0.04503(5)	0.0553(8)
S3	18f	0.307(7)	0.6293(5)	0.2982(5)	0.06703(5)	0.0616(15)
O3SA	18f	0.158(11)	0.5436(13)	0.2755(19)	0.07575(14)	0.0553(8)
O3SB	18f	0.142(10)	0.6010(19)	0.2033(13)	0.05750(14)	0.0553(8)
S4	18f	0.300(6)	-0.005(2)	-0.0256(11)	0.09660(6)	0.088(3)
O4SA	18f	0.169(11)	0.0632	-0.0619	0.1048	0.0553(8)
O4SB	18f	0.135(10)	-0.0589	-0.1188	0.0872	0.0553(8)
S5	18f	0.229(7)	0.3110(8)	0.6776(9)	0.12342(4)	0.0473(17)
O5SA	18f	0.151(11)	0.394	0.7873	0.1326	0.0553(8)
O5SB	18f	0.119(11)	0.2726	0.7297	0.1137	0.0553(8)
S6	18f	0.94(4)	0.7000(8)	0.3668(8)	0.15261(7)	0.060(3)
O6SA	18f	0.307(7)	0.7945	0.3943	0.1438	0.0553(8)
O6SB	18f	0.158(11)	0.7271	0.4598	0.1613	0.0553(8)

**Table 5a.** Selected distances of framework cations for kircherite.

Si1—O1 <sup>i</sup>	1.604(4)	Al1—O1	1.722(5)
Si1—O1 <sup>ii</sup>	1.604(4)	Al1—O1 <sup>xii</sup>	1.722(5)
Si1—O1 <sup>iii</sup>	1.619(4)	Al1—O3 <sup>xiii</sup>	1.761(4)
Si1—O1	1.619(4)	Al1—O3 <sup>xiv</sup>	1.761(4)
<Si1—O>	1.612	<Al1—O>	1.742
Si2—O4	1.611(4)	Al2—O7	1.725(4)
Si2—O3	1.599(4)	Al2—O5	1.756(5)
Si2—O5 <sup>v</sup>	1.590(5)	Al2—O4 <sup>v</sup>	1.717(4)
Si2—O6 <sup>vi</sup>	1.591(4)	Al2—O2	1.724(4)
<Si2—O>	1.598	<Al2—O>	1.731
Si3—O10 <sup>j</sup>	1.616(4)	Al3—O6 <sup>xv</sup>	1.706(5)
Si3—O9	1.623(5)	Al3—O8 <sup>xv</sup>	1.732(5)
Si3—O8 <sup>i</sup>	1.590(5)	Al3—O9	1.735(4)
Si3—O7	1.615(4)	Al3—O11	1.735(5)
<Si3—O>	1.611	<Al3—O>	1.727
Si4—O11	1.586(5)	Al4—O15 <sup>x</sup>	1.705(5)
Si4—O12 <sup>viii</sup>	1.601(6)	Al4—O13 <sup>viii</sup>	1.744(5)
Si4—O14	1.592(5)	Al4—O12	1.708(6)
Si4—O13	1.580(5)	Al4—O10	1.733(5)
<Si4—O>	1.590	<Al4—O>	1.723
Si5—O18	1.581(5)	Al5—O14	1.731(5)
Si5—O17	1.609(7)	Al5—O16	1.705(7)
Si5—O16	1.597(7)	Al5—O17 <sup>xvi</sup>	1.680(7)
Si5—O15	1.602(5)	Al5—O19	1.724(6)
<Si5—O>	1.597	<Al5—O>	1.710
Si6—O19	1.579(6)	Al6—O21	1.716(7)
Si6—O22 <sup>viii</sup>	1.577(6)	Al6—O20 <sup>iv</sup>	1.715(7)
Si6—O21	1.554(7)	Al6—O23 <sup>iii</sup>	1.689(6)
Si6—O20	1.565(6)	Al6—O18	1.695(6)
<Si6—O>	1.569	<Al6—O>	1.704
Si7—O24	1.584(7)	Al7—O22	1.710(6)
Si7—O24 <sup>ix</sup>	1.584(7)	Al7—O22 <sup>xi</sup>	1.710(6)
Si7—O23	1.571(5)	Al7—O24 <sup>xi</sup>	1.673(7)
Si7—O23 <sup>ix</sup>	1.572(5)	Al7—O24	1.673(7)
<Si7—O>	1.578	<Al7—O>	1.692

**Symmetry codes:**

(i) x-y, -y, -z; (ii) 1+x-y, 1-y, -z; (iii) x, -1+y, z; (iv) -x+y, -x, z;  
(v) 1-y, x-y, z; (vi) 1+x, y, z; (vii) 2-y, 1+x-y, z; (viii) -x+y, 1-x, z;  
(ix) 0.66667-x, 0.33333-x+y, 0.33333-z; (x) x, 1+y, z;  
(xi) -0.33333+y, 0.33333+x, 0.33333-z; (xii) -x, -x+y, -z;  
(xiii) 1-x, 1-x+y, -z; (xiv) -1+x, y, z; (xv) 1-y, 1+x-y, z; (xvi) 1-x+y, 1-x, z

**Table 5b.** Selected distances of extra-framework cations sites for kircherite.

K1-O1SB <sup>viii</sup>	2.788(6)	Na1-O1 <sup>xvii</sup>	2.648(3)	Na2A-O3XIV	2.471(5)	Ca3-O1SA	2.209(7)
K1-O2SB <sup>viii</sup>	2.800(7)	Na1-O1 <sup>xv</sup>	2.648(3)	Na2A-O3XIII	2.471(5)	Ca3-O4 <sup>xvi</sup>	2.447(3)
K1-O6	2.803(5)	Na1-O1 <sup>ii</sup>	2.648(3)	Na2A-O1SB	2.474(4)	Ca3-O4 <sup>v</sup>	2.447(3)
K1-O1SB	2.839(5)	Na1-O1 <sup>xviii</sup>	2.648(3)	Na2A-O1SBXII	2.474(4)	Ca3-O4	2.447(3)
K1-O7 <sup>x</sup>	2.840(5)	Na1-O1 <sup>xix</sup>	2.648(3)	Na2A-O2XX	2.498(4)	Ca3-O3SB <sup>v</sup>	2.586(14)
K1-O2SB	2.845(7)	Na1-O1 <sup>i</sup>	2.648(3)	Na2A-O2XXI	2.499(4)	Ca3-O3SB	2.586(14)
K1-O2 <sup>x</sup>	2.902(5)	Na1-Ow25 <sup>xx</sup>	2.709(17)	Na2A-O5XXI	2.965(3)	Ca3-O3SB <sup>xvi</sup>	2.586(14)
K1-O3 <sup>xiv</sup>	2.958(5)	Na1-Ow25	2.709(17)	Na2A-O5XX	2.965(3)	Ca3-O5	2.885(3)
K1-O1	3.216(3)	<Na1-O>	2.663	<Na2A-O>	2.602	Ca3-O5 <sup>v</sup>	2.885(3)
<K1-O>	2.888					Ca3-O5 <sup>xvi</sup>	2.885(3)
		Na5A-O4SB <sup>xxi</sup>	2.435(12)	Ca5B-O8 <sup>xviii</sup>	2.429(4)	<Ca3-O>	2.596
Na4A-O2SB <sup>viii</sup>	2.307(5)	Na5A-O4SB <sup>iv</sup>	2.435(12)	Ca5B-O8 <sup>i</sup>	2.429(4)		
Na4A-O11XV	2.498(7)	Na5A-O4SB	2.435(12)	Ca5B-O8 <sup>xv</sup>	2.429(4)	Na6A-O3SA	2.381(16)
Na4A-O10	2.504(6)	Na5A-O8X <sup>vii</sup>	2.587(6)	Ca5B-O9 <sup>iv</sup>	2.831(3)	Na6A-O14	2.422(8)
Na4A-O3SBX	2.525(15)	Na5A-O8I	2.587(6)	Ca5B-O9	2.831(3)	Na6A-O9	2.465(4)
Na4A-O6VIII	2.593(6)	Na5A-O8 <sup>xv</sup>	2.587(6)	Ca5B-O9 <sup>xxi</sup>	2.831(3)	Na6A-O4SB <sup>xxi</sup>	2.495(7)
Na4A-O7X	2.597(5)	Na5A-O9 <sup>iv</sup>	2.895(5)	Ca5B-Ow25	2.93(3)	Na6A-O15	2.512(9)
Na4A-O5X	2.672(3)	Na5A-O9	2.895(5)	Ca5B-O4S <sup>bxxi</sup>	2.976(16)	Na6A-O10 <sup>i</sup>	2.675(7)
Na4A-O12	2.914(4)	Na5A-O9 <sup>xxi</sup>	2.895(5)	Ca5B-O4SB <sup>iv</sup>	2.976(16)	Na6A-O11	2.759(8)
<Na4A-O>	2.576	<Na5A-O>	2.639	Ca5B-O4SB	2.976(16)	Na6A-O16	2.888(6)
		Na5A-Ca5B	0.622(15)	<Ca5B-O>	2.801	<Na6A-O>	2.575
Na6B-O14	2.336(17)			Na6A-Na6B	0.816(18)		
Na6B-O15	2.501(18)	K6B-O9	2.730(6)	Na6A-K6B	1.057(8)	Na7A-O2SA	2.207(9)
Na6B-O9	2.681(13)	K6B-O14	2.757(9)	K6B-Na6B	1.87(2)	Na7A-O12 <sup>xv</sup>	2.542(4)
Na6B-O16	2.952(14)	K6B-O10 <sup>i</sup>	2.776(8)			Na7A-O12	2.542(4)
Na6B-O11	2.972(18)	K6B-O11	2.826(9)	Na8C-O16V	2.583(7)	Na7A-O12 <sup>viii</sup>	2.542(4)
Na6B-O10 <sup>i</sup>	2.986(18)	K6B-O15	2.880(11)	Na8C-O16	2.583(7)	Na7A-O13 <sup>viii</sup>	2.686(4)
<Na6B-O>	2.738	K6B-O16	2.979(6)	Na8C-O16XVI	2.583(7)	Na7A-O13 <sup>xv</sup>	2.686(4)
		K6B-O3SB <sup>xvi</sup>	3.10(2)	Na8C-O6SA	2.628(9)	Na7A-O13	2.686(4)
Na8A-O16 <sup>v</sup>	2.523(6)	<K6B-O>	2.864	Na8C-O6SAXVI	2.628(9)	Na7A-O5SB	2.7255(17)
Na8A-O16 <sup>xvi</sup>	2.523(6)			Na8C-O6SAV	2.628(9)	Na7A-O5SB <sup>viii</sup>	2.7255(17)
Na8A-O16	2.523(6)	Na8B-O16 <sup>v</sup>	2.414(5)	Na8C-O17	2.868(6)	Na7A-O5SB <sup>xv</sup>	2.7255(17)
Na8A-O3SA	2.881(18)	Na8B-O16 <sup>xvi</sup>	2.414(5)	Na8C-O17V	2.868(6)	<Na7A-O>	2.607
Na8A-O3SA <sup>v</sup>	2.881(18)	Na8B-O16	2.414(6)	Na8C-O17XVI	2.868(6)		
Na8A-O3SA <sup>xvi</sup>	2.881(18)	Na8B-O17 <sup>v</sup>	2.828(6)	<Na8C-O>	2.693	Na8A-Na8B	1.063(12)
<Na8A-O>	2.702	Na8B-O17	2.828(6)			Na8A-Na8C	1.742(18)
		Na8B-O17 <sup>xvi</sup>	2.828(6)	Na9B-O19	2.49(2)	Na8B-Na8C	0.679(11)
Na9A-O4SA <sup>xxi</sup>	2.242(8)	<Na8B-O>	2.621	Na9B-O13	2.613(12)		
Na9A-O19	2.465(10)			Na9B-O18 <sup>xxi</sup>	2.66(2)	Na1K-Na1KXI	1.806(17)
Na9A-O13	2.511(5)	K9A-O19	2.727(13)	Na9B-O20	2.894(15)	Na1K-O24	2.654(7)
Na9A-O5SB <sup>xv</sup>	2.515(8)	K9A-O15 <sup>xxi</sup>	2.731(13)	<Na9B-O>	2.664	Na1K-O24XV	2.654(7)
Na9A-O18 <sup>xxi</sup>	2.624(12)	K9A-O13	2.745(8)	K9A-Na9A	0.861(9)	Na1K-O24VIII	2.654(7)
Na9A-O15 <sup>xxi</sup>	2.681(10)	K9A-O14	2.760(12)	K9A-Na9B	1.88(2)	Na1K-O5SA <sup>xv</sup>	2.701(7)
Na9A-O20	2.695(7)	K9A-O20	2.807(8)	Na9A-Na9B	1.019(18)	Na1K-O5SA	2.701(7)
Na9A-O14	2.741(9)	K9A-O18 <sup>xxi</sup>	2.909(15)			Na1K-O5SA <sup>viii</sup>	2.701(7)
<Na9A-O>	2.559	K9A-O4SB <sup>xxi</sup>	3.085(10)	Na1E-O20 <sup>xxi</sup>	2.670(10)	Na1K-O24XI	2.834(9)
		<K9A-O>	2.823	Na1E-O20 <sup>iv</sup>	2.670(10)	Na1K-O24 <sup>xxv</sup>	2.834(9)
Na1C-O20	2.563(7)			Na1E-O20	2.670(10)	Na1K-O24 <sup>ix</sup>	2.834(9)
Na1C-O20 <sup>xxi</sup>	2.563(7)	Na1D-O20 <sup>xxi</sup>	2.483(7)	Na1E-O6SB <sup>xxiii</sup>	2.703(15)	<Na1K-O>	2.730
Na1C-O20 <sup>iv</sup>	2.563(7)	Na1D-O20	2.483(7)	Na1E-O6SB <sup>xxiv</sup>	2.703(15)		
Na1C-O4SA <sup>iv</sup>	2.788(13)	Na1D-O20 <sup>iv</sup>	2.483(7)	Na1E-O6SB <sup>ix</sup>	2.703(15)	K1L-O21	2.647(9)
Na1C-O4SA	2.788(13)	Na1D-O21 <sup>iv</sup>	2.697(7)	Na1E-O21 <sup>iv</sup>	2.722(7)	K1L-O22XXV	2.735(14)
Na1C-O4SA <sup>xxi</sup>	2.788(13)	Na1D-O21	2.697(7)	Na1E-O21	2.722(7)	K1L-O21IX	2.760(11)
Na1C-O21 <sup>iv</sup>	2.938(10)	Na1D-O21 <sup>xxi</sup>	2.697(7)	Na1E-O21 <sup>xxi</sup>	2.722(7)	K1L-O23XVI	2.798(13)
Na1C-O21	2.938(10)	<Na1D-O>	2.590	<Na1E-O>	2.698	K1L-S6XXIV	2.967(15)
Na1C-O21 <sup>xxi</sup>	2.938(10)	Na1D-Na1E	0.782(18)			K1L-O23I	2.968(14)
<Na1C-O>	2.763	Na1C-Na1D	0.901(14)	Na1G-O17X	2.504(5)	K1L-O22VIII	2.991(15)
		Na1C-Na1E	1.68(3)	Na1G-O22	2.563(19)	K1L-O6SAXXIV	2.992(10)
Na1F-O5SA	2.363(8)			Na1G-O23	2.644(10)	<K1L-O>	2.857
Na1F-O6SA <sup>xxii</sup>	2.423(8)	K1G-O17 <sup>x</sup>	2.588(12)	Na1G-O24	2.724(15)		
Na1F-O17 <sup>x</sup>	2.435(9)	K1G-O24	2.676(9)	Na1G-O18X	2.737(12)	Na1L-O6SB <sup>v</sup>	2.3629(2)
Na1F-O22	2.561(15)	K1G-O22	2.684(17)	Na1G-O19XV	2.935(15)	Na1L-O6SB <sup>xxiii</sup>	2.3630(2)
Na1F-O18 <sup>x</sup>	2.597(15)	K1G-O18 <sup>x</sup>	2.718(13)	<Na1G-O>	2.685	Na1L-O21	2.502(7)
Na1F-O24	2.614(10)	K1G-O19 <sup>xv</sup>	2.738(12)			Na1L-O21 <sup>ix</sup>	2.503(7)
Na1F-O23	2.646(15)	K1G-O23	2.898(15)			Na1L-O23 <sup>i</sup>	2.638(14)
Na1F-O19 <sup>xv</sup>	2.784(15)	<K1G-O>	2.717			Na1L-O23 <sup>xvi</sup>	2.638(14)
<Na1F-O>	2.553	Na1F-Na1G	0.673(19)			Na1L-O22 <sup>viii</sup>	2.729(14)
		Na1F-K1G	0.75(2)	K1L-Na1L	1.030(10)	Na1L-O22 <sup>xxv</sup>	2.729(14)
		K1G-Na1G	1.42(3)	K1L-K1LIX	2.06(2)	<Na1L-O>	2.558

Symmetry transformations used to generate equivalent atoms:

- (I) x,y-1,z; (II) x-y+1,-y+1,-z; (III) x-y,-y,-z; (IV) -x+y,-x,z; (V) -y+1,x-y,z; (VI) x+1,y,z; (VII) -y+2,x-y+1,z; (VIII) -x+y,-x+1,z;  
 (IX) -x+2/3,-x+y+1/3,-z+1/3; (X) x,y+1,z; (XI) y-1/3,x+1/3,-z+1/3; (XII) -x,-x+y,-z; (XIII) -x+1,-x+y+1,-z; (XIV) x-1,y,z;  
 (XV) -y+1,x-y+1,z; (XVI) -x+y+1,-x+1,z; (XVII) -x,-x+y-1,-z; (XVIII) -x+y-1,-x,z; (XIX) y-1,x,-z; (XX) y,x,-z; (XXI) -y,x-y,z  
 (XXII) -x+y+1,-x+2,z; (XXIII) y-1/3,x-2/3,-z+1/3; (XXIV) x-y-1/3,-y+1/3,-z+1/3; (XXV) x-y+2/3,-y+4/3,-z+1/3; (XXVI) -x+2/3,-x+y-2/3,-z+1/3; (XXVII) -x+2/3,-x+y+4/3,-z+1/3; (XXVIII) y+2/3,x+1/3,-z+1/3; (XXIX) x-y+2/3,-y+1/3,-z+1/3



**Table 5c.** Selected distances of extra-framework anionic groups for kircherite.

S1-O1SA <sup>XX</sup>	1.461(7)	S2-O2SB	1.464(5)	S3-O3SA	1.293(16)
S1-O1SB <sup>VIII</sup>	1.466(4)	S2-O2SB <sup>VIII</sup>	1.464(5)	S3-O3SB	1.416(16)
S1-O1SB	1.466(4)	S2-O2SB <sup>XV</sup>	1.464(5)	S3-O3SA <sup>V</sup>	1.679(16)
S1-O1SB <sup>XV</sup>	1.466(4)	S2-O2SA	1.481(8)	S3-O3SB <sup>XVI</sup>	1.755(16)
<S1-O>	1.465	<S2-O>	1.468	S3-S3 <sup>V</sup>	0.809(9)
S4-O4SB	1.375(11)	S5-O5SB	1.371(4)	S6-O6SB	1.351(9)
S4-O4SA	1.42(2)	S5-O5SA <sup>XV</sup>	1.430(9)	S6-O6SA	1.370(9)
S4-O4SA <sup>IV</sup>	1.58(2)	S5-O5SA	1.547(9)	S6-O6SB <sup>XVI</sup>	1.684(10)
S4-O4SB <sup>XXI</sup>	1.67(2)	S5-O5SB <sup>XV</sup>	1.798(8)	S6-O6SA <sup>V</sup>	1.698(10)
S4-S4 <sup>XXI</sup>	0.52(2)	S5-S5 <sup>VIII</sup>	0.657(8)	S6-S6 <sup>V</sup>	0.745(14)

---

Symmetry transformations used to generate equivalent atoms:

(IV) -x+y,-x,z; (V) -y+1,x-y,z; (VIII) -x+y,-x+1,z; (X) x,y+1,z; (XI) y-1/3,x+1/3,-z+1/3;  
(XV) -y+1,x-y+1,z; (XVI) -x+y+1,-x+1,z; ; (XX) y,x,-z ; (XXI) -y,x-y,z

First revision 20/03/2012

**Table 6.** Cation site assignments on the basis of observed site scattering and geometries of the sites reported in Table 5 for kircherite

atom	Site multiplicity	Site occupancy factor	Site scattering (eps)*	Cation population (apfu)**
K1	18f	1.000	19	18 K
Na1	3a	1.000	11.0	3 Na
Na2A	9d	0.616(16)	14.5	5.54 Na + 3.46 Ca
Ca2B	9d	0.384(16)		
Ca3	6c	1.009(8)	20.2	6 Ca
Na4A	18f	0.771(12)	13.1	13.88 Na + 4.12 Ca
Ca4B	18f	0.229(12)		
Na5A	6c	0.720(14)	13.5	4.32 Na + 1.68 Ca
Ca5B	6c	0.280(14)		
Na6A	18f	0.644(9)	13.9	11.60 Na + 4.48 K +1.91 Ca
K6B	18f	0.249(4)		
Na6B	18f	0.193(8)		
Na7A	6c	0.05(2)	19.6	5.70 Ca + 0.30 Na
Ca7B	6c	0.95(2)		
Na8A	6c	0.452(15)	13.3	4.46 Na + 1.55 Ca
Na8B	6c	0.08(2)		
Na8C	6c	0.68(2)		
K9A	18f	0.236(5)	13.6	12.24 Na + 4.25 K +1.52 Ca
Na9A	18f	0.630(9)		
Na9B	18f	0.203(7)		
Na1C	6c	0.53(2)	13.3	4.46 Na + 1.54 Ca
Na1D	6c	0.18(3)		
Na1E	6c	0.50(2)		
Na1F	18f	0.23(3)	14.4	10.71 Na + 5.02 K +2.28 Ca
K1G	18f	0.411(16)		
Na1G	18f	0.367(13)		
Na1K	6c	0.516(17)	5.7	2.88 Na+ 0.12 Ca
K1L	18f	0.210(4)	4.0	3.78 K
Na1L	9d	0.580(7)	6.4	5.22 Na
Total extra framework cations (XRD)				78.62 Na + 35.53 K + 29.86 Ca
Total extra framework cations (EMPA)				89.09 Na + 18.85 K + 31.63 Ca
Ow25	6c	0.94(4)	45.1	5.64 H <sub>2</sub> O
S1	6c	1	96	6 S
S2	6c	1	96	6 S
S3	18f	0.333	96	5.04 S+0.84 Cl+0.02 F***
S4	18f	0.300(6)	88.4	4.80 S+0.40 Cl+0.46 H <sub>2</sub> O+0.12 F
S5	18f	0.229(7)	86.4	4.71 S+0.34 Cl+0.45 H <sub>2</sub> O+0.17 F
S6	18f	0.94(4)	66.0	3.51 S+0.35 Cl+0.35 H <sub>2</sub> O+0.13 F

\* eps = electrons per site, \*\*apfu (atoms per formula unit); \*\*\* We opted to assign Cl, F and excess H<sub>2</sub>O over the amount in Ow25 disordered over S3, S4,S5 and S6 because splitting off axis did not allowed to distinguish the different species. The sum < 6 apfu per site is to ascribe to the difficulty on modelling the disordering.

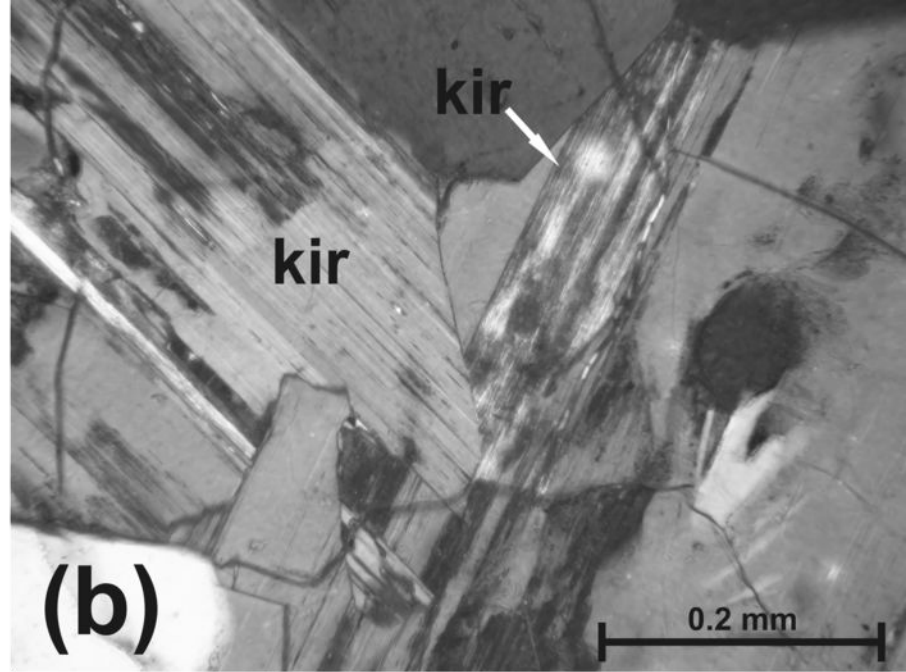
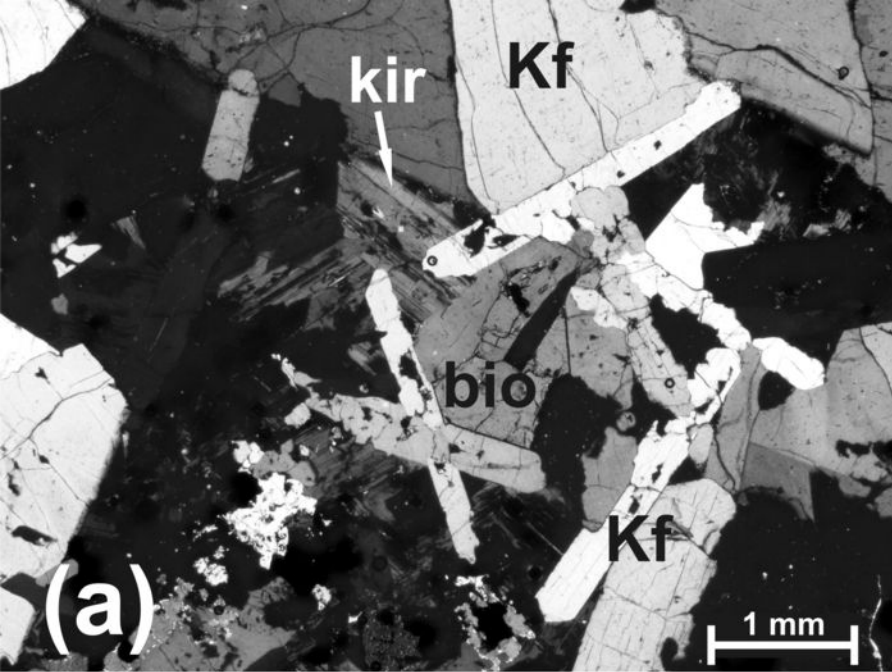


Figure 1

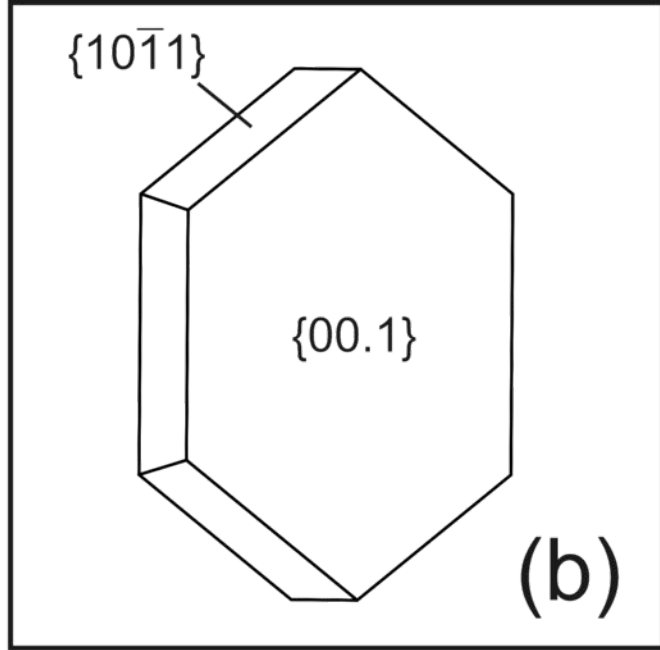
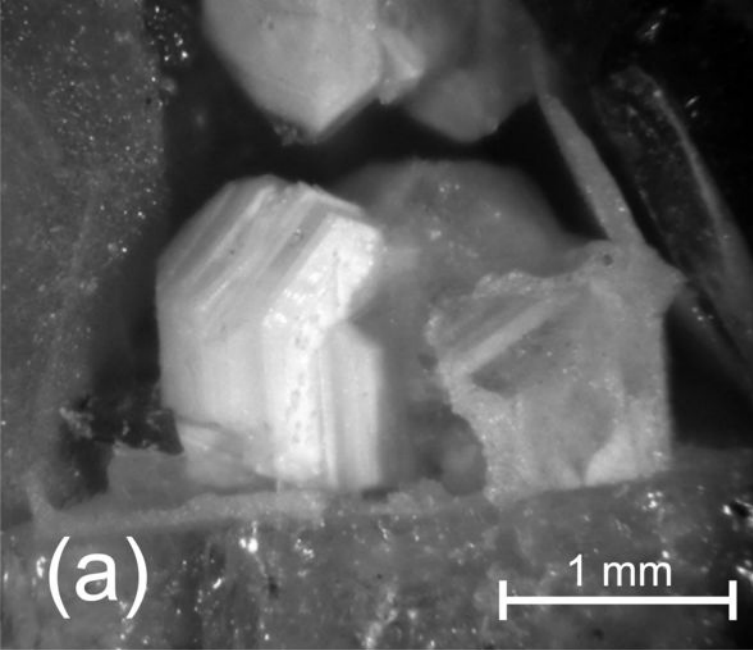


Figure 2 first revision

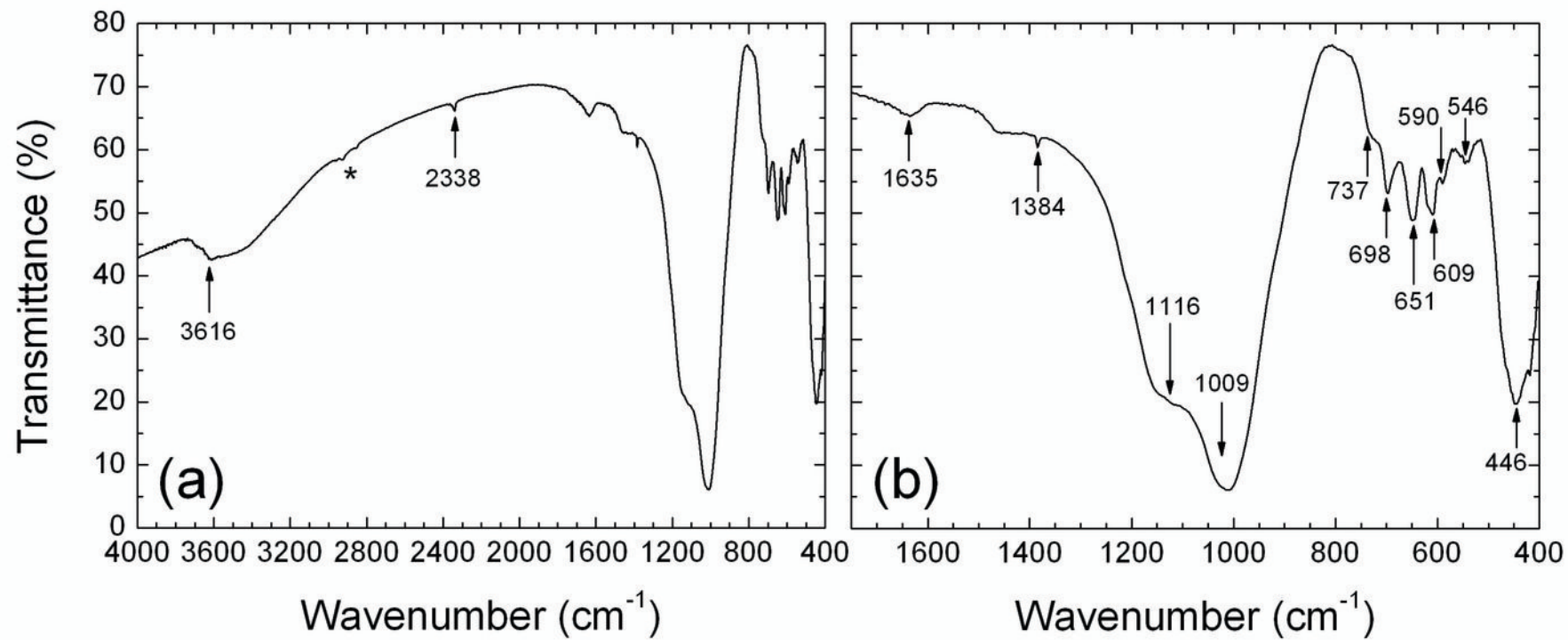


Figure 3

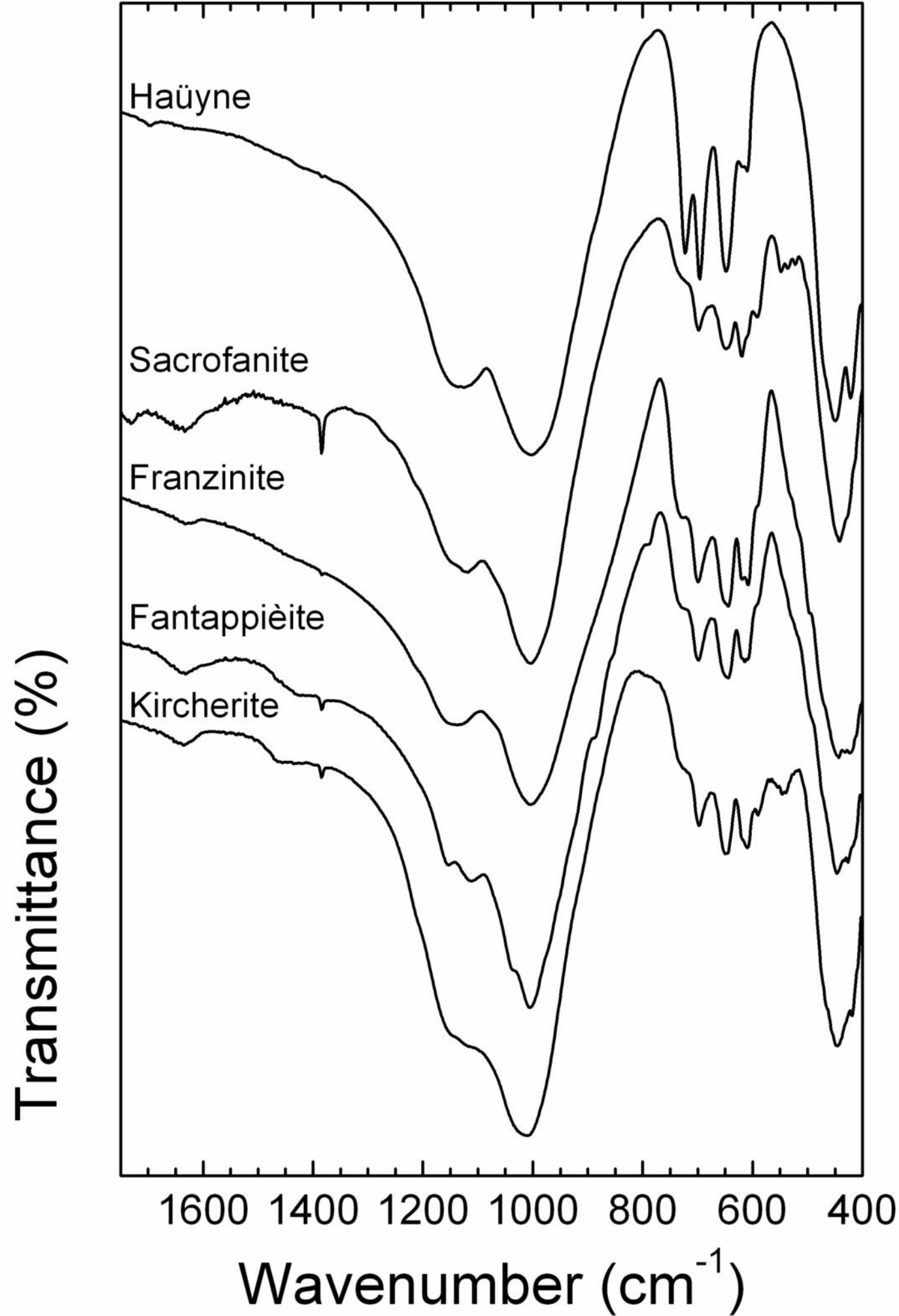


Figure 4

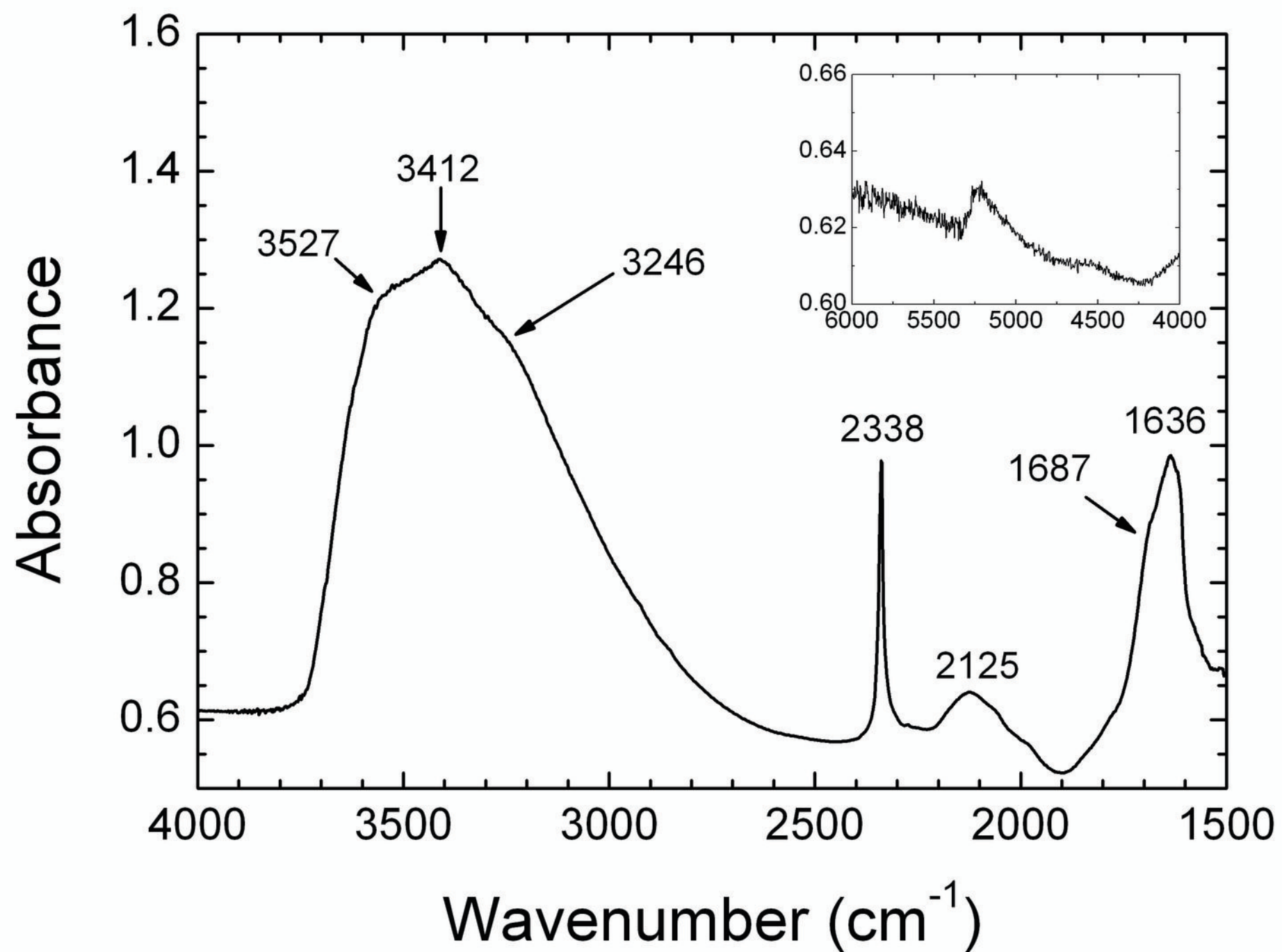


Figure 5

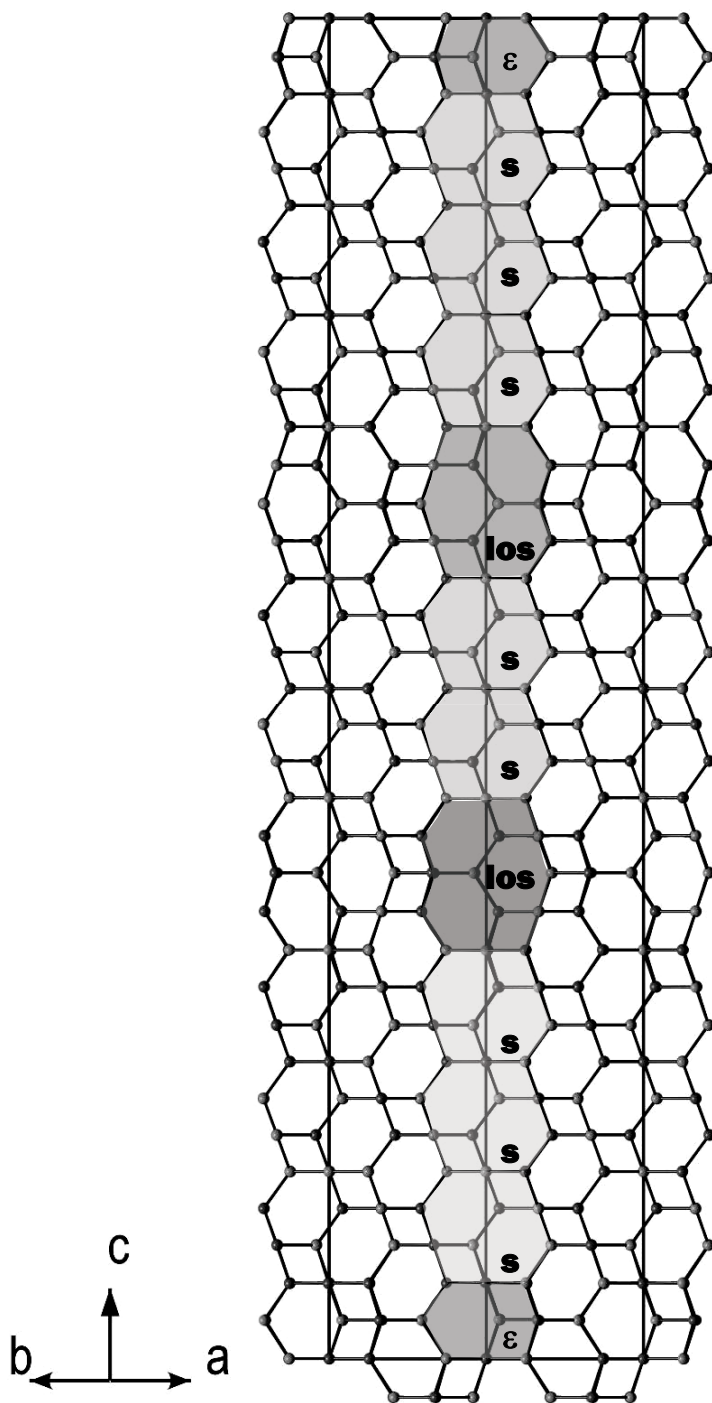


Figure 6